THERMALLY STIMULATED LUMINESCENCE AND ELECTRON SPIN RESONANCE STUDIES IN ELECTRON-IRRADIATED $CaWO_4$

By

MICHAEL DAVID SHINN

Bachelor of Science

Oklahoma State University

Stillwater, Oklahoma

1978

Submitted to the Faculty of the Graduate College
of the Oklahoma State University
in partial fulfillment of the requirements
for the Degree of
MASTER OF SCIENCE
July, 1980

THERMALLY STIMULATED LUMINESCENCE AND ELECTRON SPIN RESONANCE STUDIES IN ELECTRON-IRRADIATED $CaWO_4$

Thesis Approval:

Thesis Adviser

Larry E. Halliburton

Dean of the Graduate College

ACKNOWLEDGMENTS

I would like to thank my thesis advisor, Dr. Elton Kohnke, for the many discussions we had in the course of doing the research which led to this thesis. These discussions have led me to adopt a more realistic view of the application of theoretical models to experimental results. Special thanks go to Dr. Larry Halliburton, who served as a "second thesis advisor" of sorts, and who also helped interpret the ESR spectra and had the patience to help me learn the basics of ESR techniques. My thanks also to Dr. Geoffrey Summers, who served on my Master's Committee, and made many helpful suggestions which improved this thesis.

I am fortunate to be working in a department with many good people, and wish to express my gratitude to Drs. William Sibley, Joel Martin, and George Dixon for their helpful discussion and suggestions, and to Dr. Richard Powell, for suggesting I do research on $CaWO_4$ and for being so generous with his crystals. My thanks also to Dr. Mark Markes, who helped me take some of the ESR data even when it meant staying up late, and for helping with some of the analysis. To my friends Mahendra Jani, and Bryce Jeffries goes my gratitude for letting me use them as a sounding board for my ideas.

Janet Sallee, who has been a friend for many years, has done a masterful job of typing this thesis. I appreciate her hard work.

Financial support, provided under the form of a Research Assistantship by the Radiation Safety Program, is greatly appreciated.

My sincere thanks go to my parents for their years of love and encouragement, and their support, both psychological and financial, as well. And finally, to Helen Mary, my appreciation for her understanding and encouragement while writing this thesis.

TABLE OF CONTENTS

TABLE

LIST OF FIGURES

CHAPTER I

INTRODUCTION

Calcium tungstate ($CaWO_4$), or scheelite, has a structure which provides a model for all other scheelite-structured crystals. The atoms do not all bind ionically to one another, as in the alkali halides. Instead the oxygen atoms bind covalently to the tungsten atom, producing a WO_4^{2-} molecular complex which itself binds ionically to the Ca^{2+} ion. The unit cell is shown in Figure 1, and has the dimensions $a = b = 5.24\text{Å}$ and $c = 11.37\text{Å}$ (1). Optical absorption data indicates a sharp absorption at about 300 nm with a slight absorption to 500 nm. Hence the band gap is about 4.1 eV. It has been known for some time that powdered $CaWO_4$ is an excellent phosphor, producing a blue luminescence when exposed to ultraviolet and x-ray photons or fast electrons. Kröger (2) found that all the tungstates which do luminesce do so in this spectral region and concluded that the luminescence is due to electronic transitions within the $(WO_4)^{2-}$ complex.

$CaWO_4$ has been used commercially, primarily for x-ray fluorescent screens. It has also been used for u.v.-sensitive photomultiplier tubes and for photo-electric cells. When doped with neodymium, $CaWO_4$ becomes the host material for an infrared laser.

Concurrent with research on the luminescence of $CaWO_4$ has been research into its radiation-induced defects. Two experimental methods used in this research are thermally stimulated luminescence (TSL) and electron spin resonance (ESR) and these are the areas of interest in the present study.

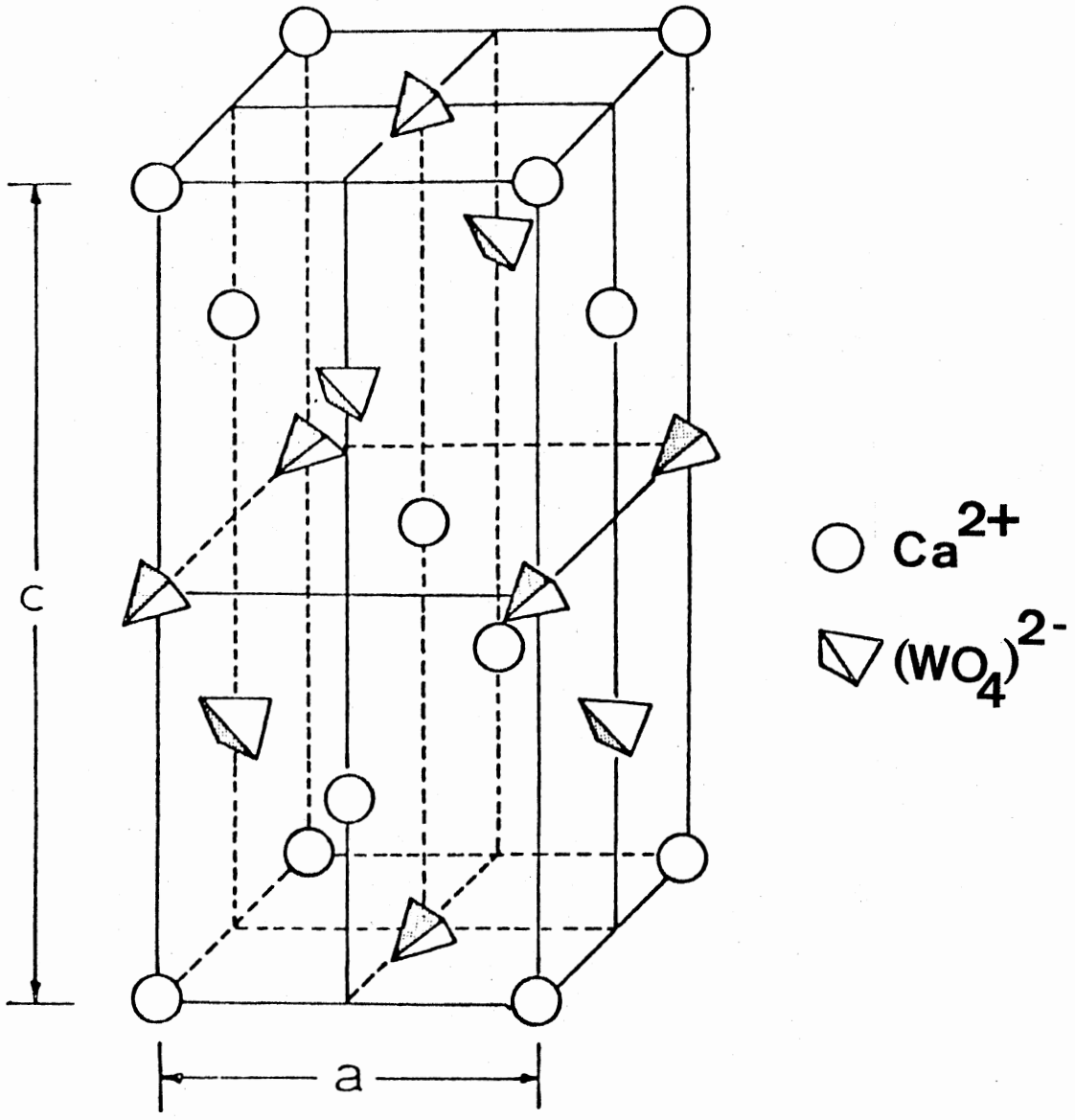

Figure 1. Scheelite Structure of $CaWO_4$

The TSL of $CaWO_4$ has been studied since the late 1950's. Sayer and Souder (3) have summarized the published data on the glow peak temperatures found for nominally pure $CaWO_4$ after various types of excitation. The data may be placed in groups. These groups are: 110-119°K, 126-136°K, 154°K, 210-225°K, 257-270°K, 290-300°K, and 325°K. The same paper also contains the results of their studies on the TSL of doped and nominally pure $CaWO_4$ single crystals irradiated by u.v. or x-ray sources. Their results suggest that monovalent impurities enhanced the 154°K TSL peak normally associated with radiation damage, creating a TSL peak of complex shape at 160°K and producing a peak at 260°K. The effect of trivalent impurities was less pronounced on the 160°K peak, but enhanced production of glow peaks at 220°K and at 300°K. The TSL had a spectrum which peaked at 420 nm.

The authors suggest the following structures for the observed TSL: 154/160°K - oxygen vacancies associated with either a W^{5+} or a monovalent ion at a calcium site, 260°K-monovalent ions at calcium sites, 300°K-calcium vacancies.

A pioneering work on the ESR of $CaWO_4$ was done by Zeldes and Livingston (4). Gamma irradiation at 77°K was found to have produced two paramagnetic species. Interpretation of the hyperfine effects for one indicate that a hole is situated between two tungsten nuclei, probably in the outer oxygen ions, while the other paramagnetic center is an electron situated near a tungsten atom. This species could be $(WO_4)^{3-}$, but from the lack of symmetry the authors believe that the electron center must be near a lattice defect.

A large amount of work correlating ESR and TSL has been done at the Physikalisches Institut, University of Giessen, under the supervision of Dr. A. O. Scharmann (5-7). They reported that nominally pure

$CaWO_4$, irradiated at liquid air temperature with x-rays, shows one broad TSL peak centered at 225°K. The ESR measurements show a broad signal due to electrons trapped at defects and a set of lines which are interpreted as being a hole trapped between two tungstate tetrahedra. At liquid nitrogen temperature the electron is shared equally and becomes more localized on one tetrahedron only when the temperature approaches liquid helium temperature. This hole is somewhat analogous to the V_k center in the alkali halides and operating on this assumption, the authors discuss the TSL in terms of a small polaron model. Below 150°K the traps containing the electrons and the polarons are spatially separated. In this temperature range the polaron can only move by tunneling so this separation keeps the probability of recombination low. Above 150°K the polaron moves by "hopping" from one site to an equivalent site making the probability of recombination high. When recombination occurs TSL results.

Work by Koehler and Kikuchi (8) on the TSL and ESR of $CaWO_4$ irradiated by gamma rays at 78°K supports a different model. Warming after irradiation produces three TSL peaks at 155°K, 225°K, and 290°K. All three peaks' emissions were spectrally centered at 490 nm. The ESR spectra is interpreted to be two sets of lines due to W^{5+} and lines due to Nb^{4+}. Different saturation curves on the W^{5+} lines lead the authors to the conclusion that there must be two independently trapped sets of electrons. Their interpretation is that WO_3 substituting for $(WO_4)^{2-}$, creating an oxygen vacancy, is responsible for the two W^{5+} centers. The 155°K peak is due to a $(WO_4)^{3-}$ complex near a WO_3 molecule and a $(NbO_4)^{3-}$ radical. The 225°K peak is due to a $(WO_3)^{1-}$ complex with a nearby calcium vacancy. The 290°K peak is then due to Nb^{4+} in a tungsten site, which forms the $(NbO_4)^{3-}$ mentioned above.

It is clear that a model for the observed TSL in $CaWO_4$ has not been firmly established. The purpose of this thesis is to report our results of TSL and ESR measurements on $CaWO_4$ irradiated with fast electrons. By correlating experiments using these two methods, a model for the radiation-induced defects which produces the observed effects may be proposed.

CHAPTER II

THEORETICAL DISCUSSION

TSL Theory

Thermally stimulated luminescence (TSL) is the emission of light by a material at a temperature below that of incandescence. It is a phenomenon which is exhibited by many materials, both inorganic and organic. TSL has been known to scientists for centuries. A report by Sir Robert Boyle on a diamond which glowed in the dark when warmed appeared in 1663. However, no good theory of TSL was developed until the late 1930's, with the development of band theory.

Qualitatively, one may explain TSL by considering the effect of defects in a crystal. The defects will often create localized regions where an electron or hole may be trapped, having an energy intermediate in comparison to the difference in the conduction and valence band energies. Initially such a crystal has a filled valence band, with no electrons in the conduction band or trapped at a defect. If ionizing radiation is then incident on the crystal electrons will be excited out of the valence band into the conduction band, leaving a hole behind. The electron and hole may then recombine, producing luminescence, or they may both be trapped at spatially separated points in the crystal, often at one of the defects. The electron and hole stays trapped until one or the other can gain enough energy to become untrapped. To simplify discussion suppose it is the electron which becomes untrapped. This occurs when it can gain enough energy to move back into the conduction band. The place where it was trapped is then called the trapping

center. The untrapping process can occur by heating the crystal, since energy may be supplied by the interaction of phonons with the electron. Once in the conduction band the electron may be retrapped or may migrate to the center where the hole is trapped and emit a photon as the electron and hole recombine. The center where the hole is trapped is then called a recombination center. This emission of light is TSL.

When the hole becomes untrapped first, the assignment of trapping and recombination centers is reversed, but the mechanism is essentially the same. Normally one obtains data which gives the TSL intensity as a function of temperature, the resulting data is commonly called a glow curve.

It should be noted that several assumptions were made in the above discussion. They are:

1) Each glow curve corresponds to the release of trapped charges from a discrete energy level in the band gap.

2) The TSL intensity is proportional to the rate of recombination of the charge with the luminescent center.

3) The excited state of the luminescent center is near the bottom of the conduction band (for electrons).

4) When a charge is untrapped it may only be retrapped or recombine to produce TSL.

A band model using these assumptions is shown in Figure 2. Arrows show the directions of the transitions. The symbols next to the arrows have the following meanings:

α = the probability of excitation into the conduction band.

β = the probability of retrapping the electron.

γ = the probability of recombination at a recombination center.

To derive formulae which produce quantitative results the following

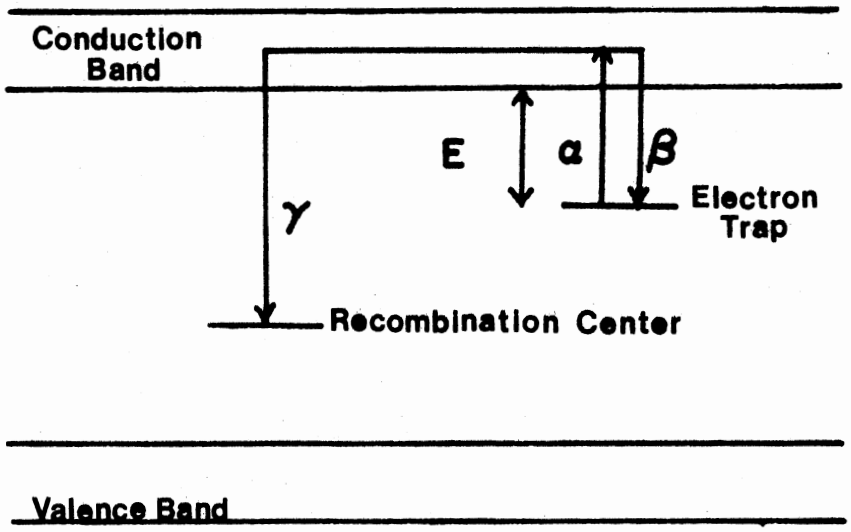

Figure 2. Band Model for TSL

quantities are defined:

n = the concentration of electrons in the conduction band.

h = the concentration of trapped electrons.

H = the concentration of trapping centers.

f = the concentration of recombination centers.

γnf = the number of recombination transitions occurring per unit volume per unit time.

αh = the number of transitions into the conduction band occurring per unit volume per unit time.

$\beta n(H-h)$ = the number of retrapping transitions occurring per unit volume per unit time.

The rate of change of free electrons with time is:

$$\frac{dn}{dt} = \alpha h - \beta n(H-h) - \gamma nf \tag{1}$$

The rate of change of trapped electrons with time is:

$$\frac{dh}{dt} = -\alpha h + \beta n(H-h) \tag{2}$$

The rate of change of recombination centers with time is:

$$\frac{df}{dt} = -\gamma nf \tag{3}$$

Since the crystal must remain electrically neutral the following equation must also hold true:

$$f = n + h \tag{4}$$

At any given time the mean lifetime of trapped electrons is long so $h >> n$. This implies:

$$f \approx h \qquad \frac{df}{dt} \approx \frac{dh}{dt}$$

Before proceeding further an important assumption regarding the dependence of α on temperature must be made. Since the recombination process is thermally activated the most reasonable assumption is:

$$\alpha = \alpha_o \exp(\frac{-E}{kT}) \tag{5}$$

where k is Boltzmann's constant and E is the activation energy, i.e., the energy difference between the trapping level and the conduction band. The symbol α_o is the pre-exponential factor. To have the intensity dependent on the temperature, rather than the time, one uses the relation:

$$dT = qdt \tag{6}$$

where q is the constant heating rate.

The intensity of the luminescence is given by:

$$I = \gamma nf = -\frac{df}{dt} = -\frac{dh}{dt} \tag{7}$$

as long as the condition $h >> n$ is true.

Normally (7) is solved in two special cases. The first case assumes no retrapping, so $\beta = 0$. This is called first-order kinetics and was first solved by Randall and Wilkins (9). The other case assumes that retrapping and recombination probabilities are equal. This is called second-order kinetics and was first solved by Garlick and Gibson (10). Considering first-order kinetics first, if $\beta = 0$ then (2) becomes:

$$-\frac{dh}{dt} = \alpha h \tag{8}$$

or,

$$\frac{dh}{h} = -\alpha dt = -\frac{\alpha}{q} dT \tag{9}$$

Integrating from some temperature T_o, when $h = h_o$, to a temperature T, when $h = h$:

$$\int_{h_o}^{h} \frac{dh'}{h'} = -\int_{T_o}^{T} \frac{\alpha}{q}\, dT' \tag{10}$$

$$\ln h' \Big|_{h_o}^{h} = -\int_{T_o}^{T} \frac{\alpha}{q}\, dT' \tag{11}$$

$$\frac{h}{h_o} = \exp\left[-\int_{T_o}^{T} \frac{\alpha}{q}\, dT'\right] \tag{12}$$

Using (5) for α:

$$h = h_o \exp\left[-\frac{\alpha_o}{q}\int_{T_o}^{T} \exp\left(\frac{-E}{kT'}\right) dT'\right] \tag{13}$$

Since, from (7) and (8), $I = \alpha h$, then:

$$I = \alpha_o h_o \exp\left[\frac{-E}{kT} - \frac{\alpha_o}{q}\int_{T_o}^{T} \exp\left(\frac{-E}{kT'}\right) dT'\right] \tag{14}$$

A plot of I versus T, using (14) is shown in Figure 3.

In the case of second-order kinetics the retrapping rate β is equal to the recombination rate γ. Since there are H-h empty traps and h available recombination centers at any time the probability of recombination is given by:

$$\frac{ch}{[(H-h)+h]} = \frac{ch}{H} = \gamma \tag{15}$$

where c is a constant of proportionality. Now (7) is written:

$$I = \gamma nf = -\frac{dh}{dt} = \alpha h - \beta n(H-h) \tag{16}$$

Since $\gamma = \beta$ and $f << h$ (16) becomes, using (15):

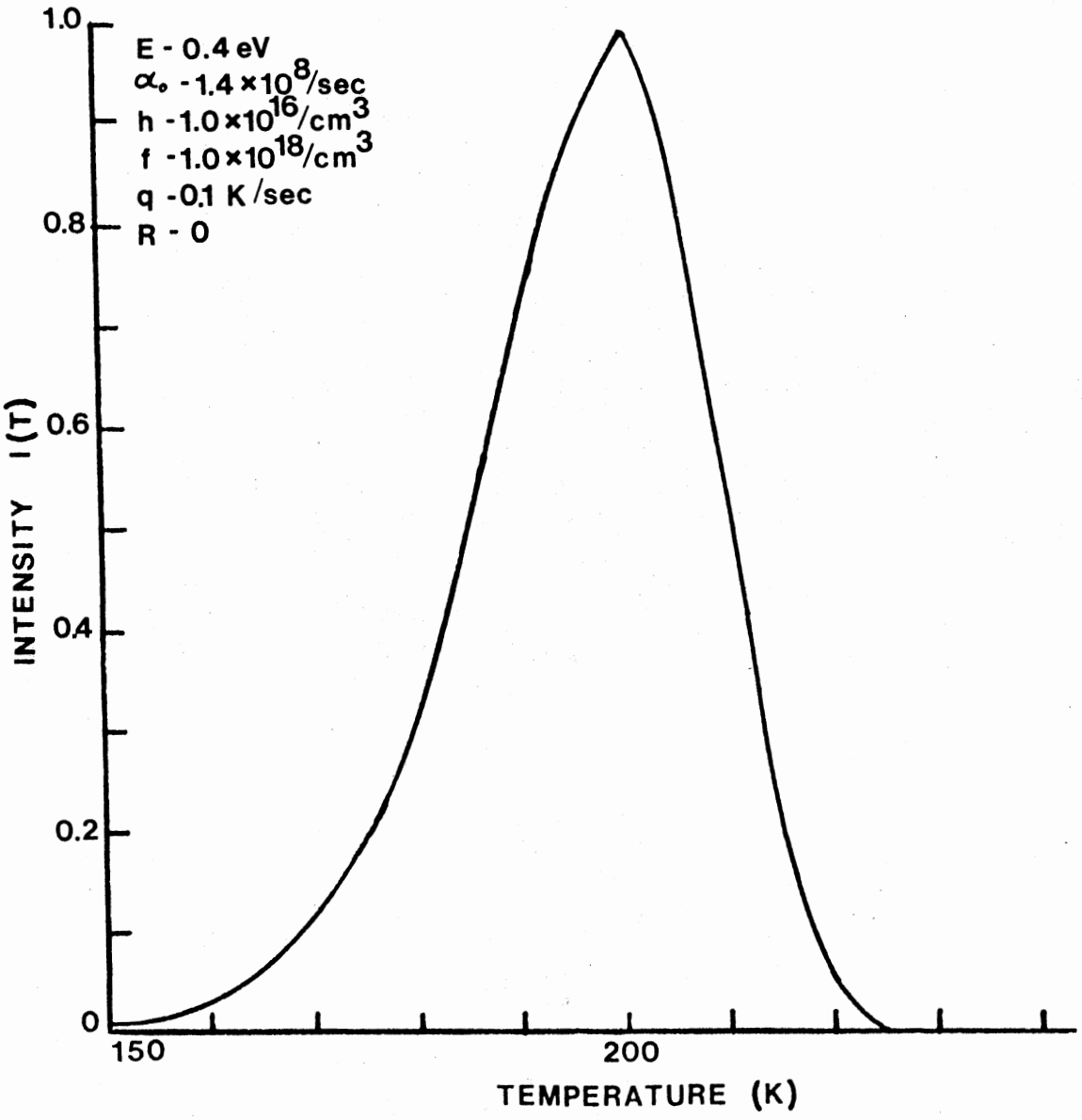

Figure 3. Plot of I Versus T for 1st Order Kinetics

$$\frac{ch}{H}\, nh = \alpha h - \frac{ch}{H}\, n(H-h) \tag{17}$$

$$\frac{cnh^2}{H} = \alpha h - cnh + \frac{cnh^2}{H} \tag{18}$$

or,

$$nh = \frac{\alpha h}{c} \tag{19}$$

Substituting (19) into (18), and using (15):

$$I = \gamma nh = \frac{\gamma \alpha h}{c} = \frac{\alpha h^2}{H} = -\frac{dh}{dt} \tag{20}$$

This may be written:

$$\frac{dh}{h^2} = \frac{\alpha}{H}\, dt = \frac{-\alpha}{qH}\, dT \tag{21}$$

Integrating over the same limits as in the first case:

$$\int_{h_o}^{h} \frac{dh'}{h'^2} = \frac{-1}{qH} \int_{T_o}^{T} \alpha dT' \tag{22}$$

$$-\frac{1}{h'}\Big|_{h_o}^{h} = \frac{-\alpha_o}{qH} \int_{T_o}^{T} \exp\left(\frac{-E}{kT'}\right) dT' \tag{23}$$

$$-\frac{1}{h} = -\left(\frac{1}{h_o} + \frac{\alpha_o}{qH} \int_{T_o}^{T} \exp\left(\frac{-E}{kT'}\right) dT'\right) \tag{24}$$

so

$$h = \left[\frac{1}{h_o} + \frac{\alpha_o}{qH} \int_{T_o}^{T} \exp\left(\frac{-E}{kT'}\right) dT'\right]^{-1} \tag{25}$$

Substituting into (20):

$$I = \frac{\alpha h^2}{H} = \frac{\alpha_o h_o^2 \exp(\frac{-E}{kT})}{H[1 + \frac{\alpha_o h_o}{qH} \int_{T_o}^{T} \exp(\frac{-E}{kT'}) dT']^2} \quad (26)$$

A plot of I versus T, using (26) is shown in Figure 4. Comparison of these two cases with experimental data shows that either method gives approximately the right shape of the data curves. In the literature one may find methods purporting to determine the order of the kinetics and, by curve-fitting, to determine α_o and E as well. However, one must be careful in interpreting the numbers obtained since in many cases the initial assumptions may not be valid. The same may be said for the simplifying assumptions used to obtain exact solutions of the rate equations. A definitive paper by Kelly, Laubitz, and Bräunlich (11) established the a priori knowledge of the model and parameters n, h, H, and f as essential before an unambiguous determination of α_o and E can be made. They stated that:

> We are convinced that analyses of thermally stimulated processes can only be meaningful if the defect structure of the solid is known so that a realistic model may be constructed, and if some of the associated parameters, such as mobility and luminous efficiency, as well as the band structure, are reasonably well known as functions of temperature. Then, and only then, will analyses of TSC and TSL provide useful and unambiguous information of the trapping parameters (p. 1967).

To help determine the mechanism of the observed TSL, i.e., the traps and recombination centers, another sensitive technique, electron spin resonance, was used. The next section explains the theory used in interpreting ESR data.

ESR Theory

Compared to TSL, electron spin resonance (ESR) has a brief history. The first successful ESR experiment was performed by

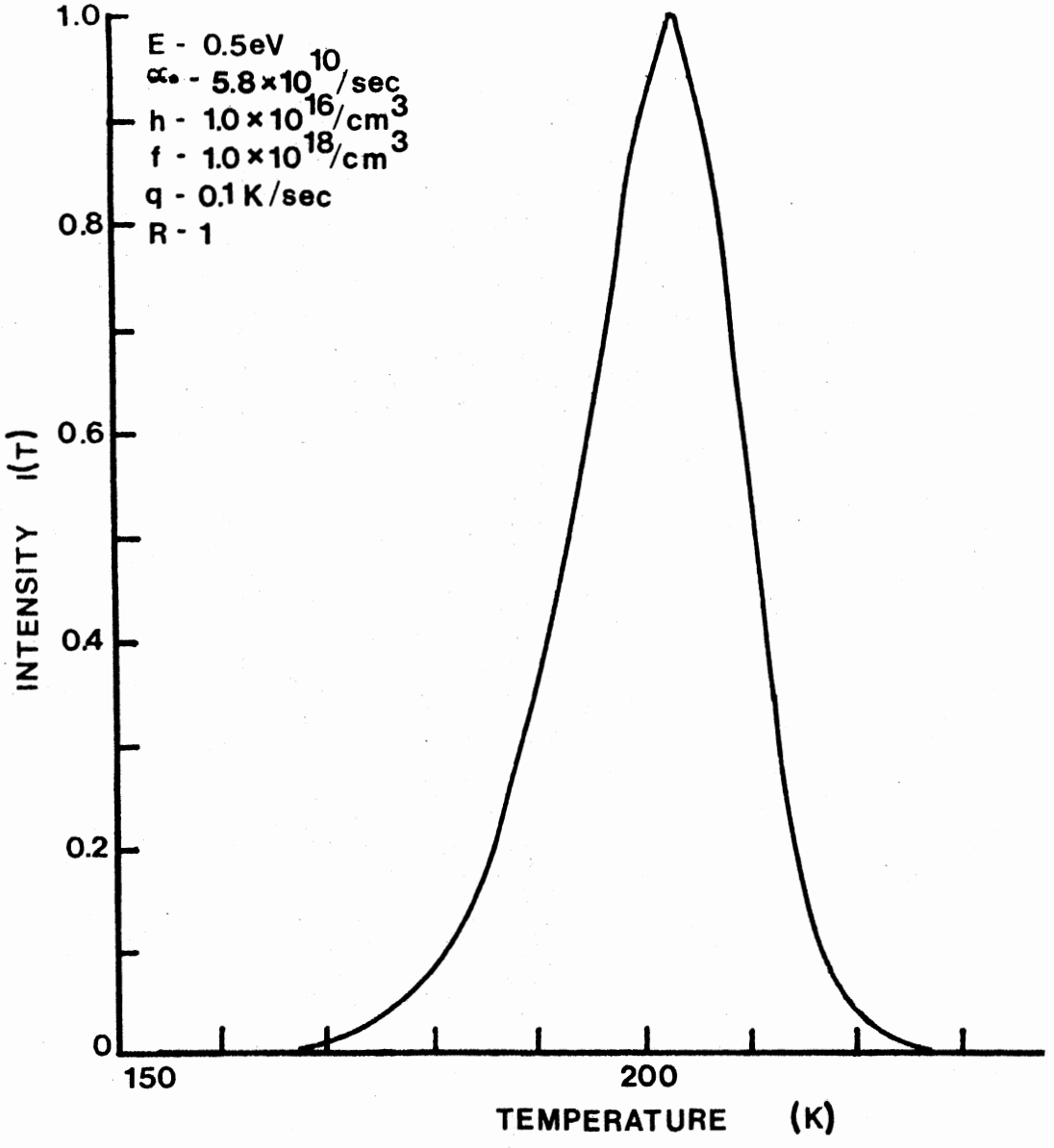

Figure 4. Plot of I Versus T for 2nd Order Kinetics

E. Zavoisky of the USSR in 1944. Since then it has been applied to substances over a wide range of temperatures by experimenters in the physical and biological sciences.

Crucial to the development of ESR was the discovery in 1921 by Stern and Gerlach that the electron possessed a quantized intrinsic angular momentum, which is called the electron spin. The angular momentum may be related to the magnetic moment by the equation:

$$\mu = - g\beta M_s \tag{27}$$

β is the Bohr magneton, and μ is the magnetic moment. The "g-factor", represented by g, is a factor required in all cases where the magnetic moment is not solely due to orbital angular momentum. Thus a paramagnetic atom or ion will have the degeneracy of the ground state removed when it is placed in a magnetic field. If the magnetic field intensity is H, then the magnitude of the splitting of the ground state is given by:

$$W = g\beta H \tag{28}$$

and thus increases linearly as H is increased, as shown in Figure 5.

If an electromagnetic wave of frequency ν is applied so the magnetic field component is perpendicular to H and:

$$h\nu = g\beta H \tag{29}$$

then a magnetic dipole transition will occur between the two levels. This is called the resonance condition and corresponds classically to flipping the electron's spin. The resonance condition is an example of the selection rule for "allowed" transitions: for allowed transitions to occur the condition:

$$\Delta M_s = \pm 1 \tag{30}$$

must hold. For a system of paramagnetic atoms or ions in thermal

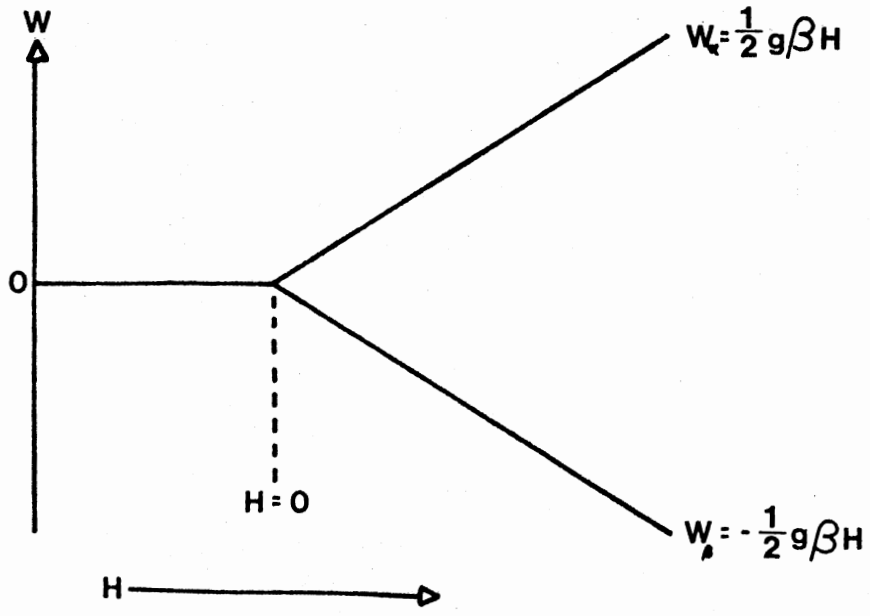

Figure 5. Energy Level Splitting for $S = \frac{1}{2}$ System

equilibrium the ratio of the electron population with spin $+\frac{1}{2}$ to the electron population with spin $-\frac{1}{2}$ is equal to the Boltzmann factor:

$$\frac{n(+\frac{1}{2})}{n(-\frac{1}{2})} = \exp(\frac{-W}{kT}) \qquad (31)$$

so at most temperatures of interest there are far more electrons in the lower energy level. The resonance condition is found by fixing the photon energy and varying the magnetic field. When fulfilled, the transitions to the higher energy level result in an absorption which may be detected. Once ν and H are known one can solve for g to find the "g-factor" for the particular paramagnetic system.

If this were the only parameter measured ESR would provide rather limited information. In many systems the so-called "hyperfine splitting" gives additional information which allows the experimenter to determine the paramagnetic species. This is due to nuclei which possess an intrinsic angular momentum. The spin quantum number I of these magnetic nuclei takes on one of the values I = $\frac{1}{2}$, 1, $\frac{3}{2}$, 2, ... etc., with a corresponding multiplicity of spin states given by (2I+1). These nuclei perturb the magnetic field experienced by the electron, which changes the resonance condition so there are (2I+1) absorptions. Since I is known for all nuclei this often makes identification of a particular paramagnetic species possible. An example of the energy levels of an S = $\frac{1}{2}$ I = $\frac{1}{2}$ system is shown in Figure 6.

One might think that problems would arise from distinguishing one I = 0, S = $\frac{1}{2}$ system from another, since only one ESR absorption line results from such systems. Often a paramagnetic species with I = 0 has one or more naturally occurring isotopes with $I \neq 0$. The spectrum which results will consist of the absorption due to the I = 0, S = $\frac{1}{2}$ system with 2I+1 hyperfine lines due to each of the isotopes symmetrically spaced about it. Such a spectrum will have the property that the ratio

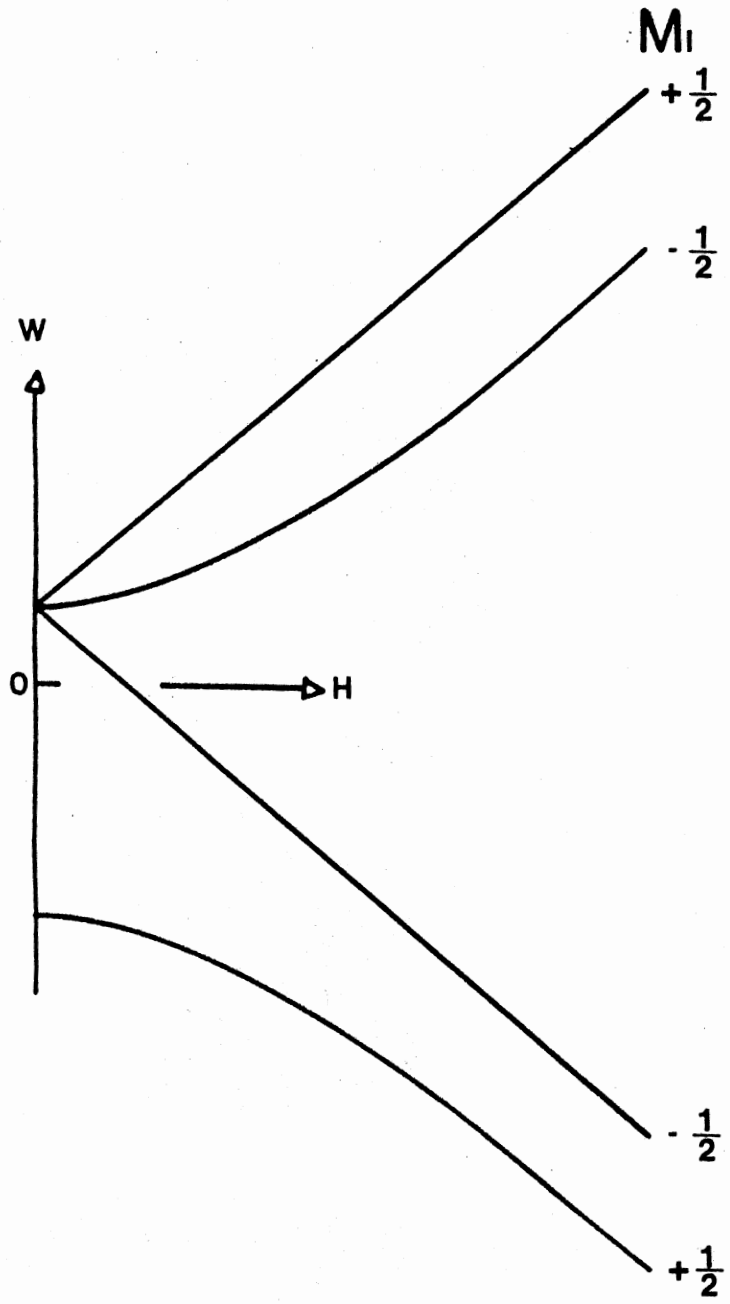

Figure 6. Energy Level Splitting for $I = \frac{1}{2}$, $S = \frac{1}{2}$ System

of the sum of the peak-to-peak amplitudes of the first derivative of the hyperfine absorptions to the peak-to-peak amplitude of the first derivative of the I = 0 absorption will be equal to the ratio of their isotopic abundances. Thus a paramagnetic species may be positively identified by an application of these various analysis techniques to the ESR data.

ESR is useful in solid state physics because of the ability it has in determining the identity of paramagnetic defects in crystals. ESR is able to detect as few as 10^{12} ions/cm^3 in a host crystal, which is about the number of recombination centers needed to observe TSL. In principle then, ESR should provide information on the mechanism of TSL in crystals.

It should be noted that the examples given above are for simple systems. In general, S is of half-integer value greater than one half, transitions may occur between "forbidden" levels, interactions with surrounding nuclei other than the paramagnetic species' nuclei may occur; all these effects and others will complicate the ESR spectrum. For more information, consult any of the texts on ESR theory.

CHAPTER III

EXPERIMENTAL APPARATUS AND PROCEDURE

TSL Apparatus

A diagram of the TSL apparatus is shown in Figure 7. The light emitted by the sample is monitored from both sides. On one side the light passes through a quartz window of the cryostat and is detected by an EMI 9558Q photomultiplier tube operated at 1000 V and powered by a Hamner Electronics Corporation N-401 power supply. This tube has an S-20 response which is most sensitive around 400 nm. The output of the phototube is connected to a Keithley Model 602 electrometer and the output of the electrometer is connected to the Y-axis of a Houston Instruments Model 2000 X-Y recorder. A copper-constantan thermocouple, which monitored the sample temperature, was connected to the X-axis of the recorder.

Light from the other side of the sample is analyzed by a Bausch and Lomb 0.5 meter monochromator with a linear dispersion of 1.6 nm per millimeter and 1.5 mm slits and is detected by an RCA C31034 photomultiplier tube operated at 1500V by a Keithley 244 power supply and cooled to -30^{o}C by a water-cooled Pacific Photometric Institute Thermoelectric photomultiplier housing, model 3463, powered by a power supply/temperature controller model 33. The signal from the photomultiplier tube is sent to a Keithley Model 600B electrometer and the output of the electrometer is filtered and connected to the Y-axis of a Moseley Model 25 X-Y recorder. The X-axis is connected to a power supply built in our lab by Mr. Dost Malik. The voltage applied to the X-axis is

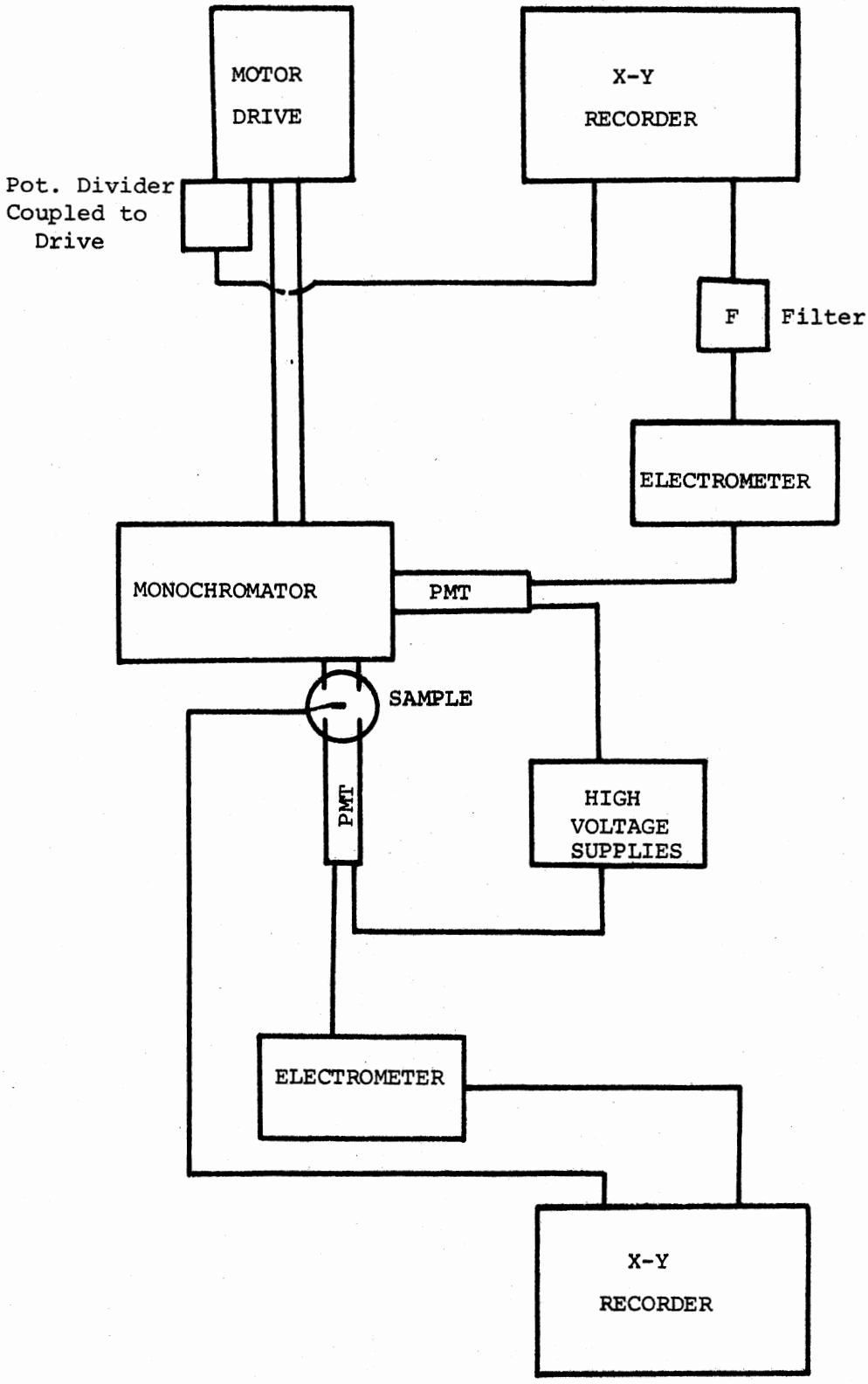

Figure 7. Diagram of TSL Apparatus

potentiometrically varied using a gearing attachment which senses the rotation of the monochromator drive, providing a direct plot of luminescence intensity as a function of wavelength.

The filter used deserves some special mention since it was custom-built in this lab. The light emitted at the output of the monochromator is of very low intensity, and the resultant photocurrent is often only two or three times greater than the dark current, which is about 5×10^{-12} amperes. Hence the signal is very noisy. Since the type of experiment done precludes the use of signal averaging a decision was made to use signal bandwidth filtering. The filter design was suggested by D. F. Stout and is a low pass active filter schematically diagrammed in Figure 8. The values shown in the schematic make the filter a unity gain device with an 18 db/octave rolloff above 0.5 Hz. This filter significantly reduces the noise in the phototube output without the annoying time constant effects of passive RC filters.

The cryostat used is pictured on the next page and was custom built at Oklahoma State University (Figure 9). The sample is held to the copper cold finger of the cryostat by a copper plate fastened with brass screws. Soft indium foil is placed between the sample and the copper surfaces to improve the thermal contact. Matched rectangular cutouts with dimensions of 6mm x 12mm in both the cold finger and the copper plate allowed observations of the luminescence. The sample and cold finger are surrounded by a cylindrical copper radiation shield with optical cutouts. The base of the cryostat may be rotated and contains three quartz windows and one aluminum window. The cold finger is coupled to the cryogenic fluid reservoir through a combination copper-stainless steel shank. The copper-constantant thermocouple is silver soldered to a hole drilled in the cold finger with the reference junction main-

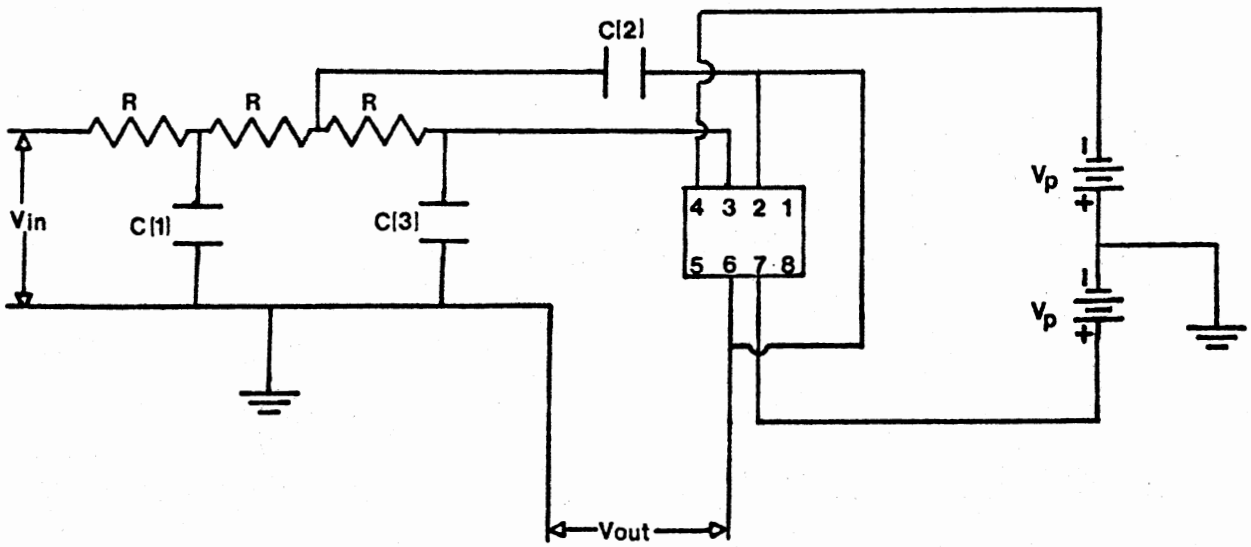

R–196 KΩ
C[1]–3.3 uF
C[2]–10 uF
C[3]–180 uF
Vp–9V
OP AMP–741

OFFSET NULL	1	8	NC
INVERTING INPUT	2	7	V+
NONINVERTING INPUT	3	6	OUTPUT
V-	4	5	OFFSET NULL

Figure 8. Schematic of 0.5 Hz Filter

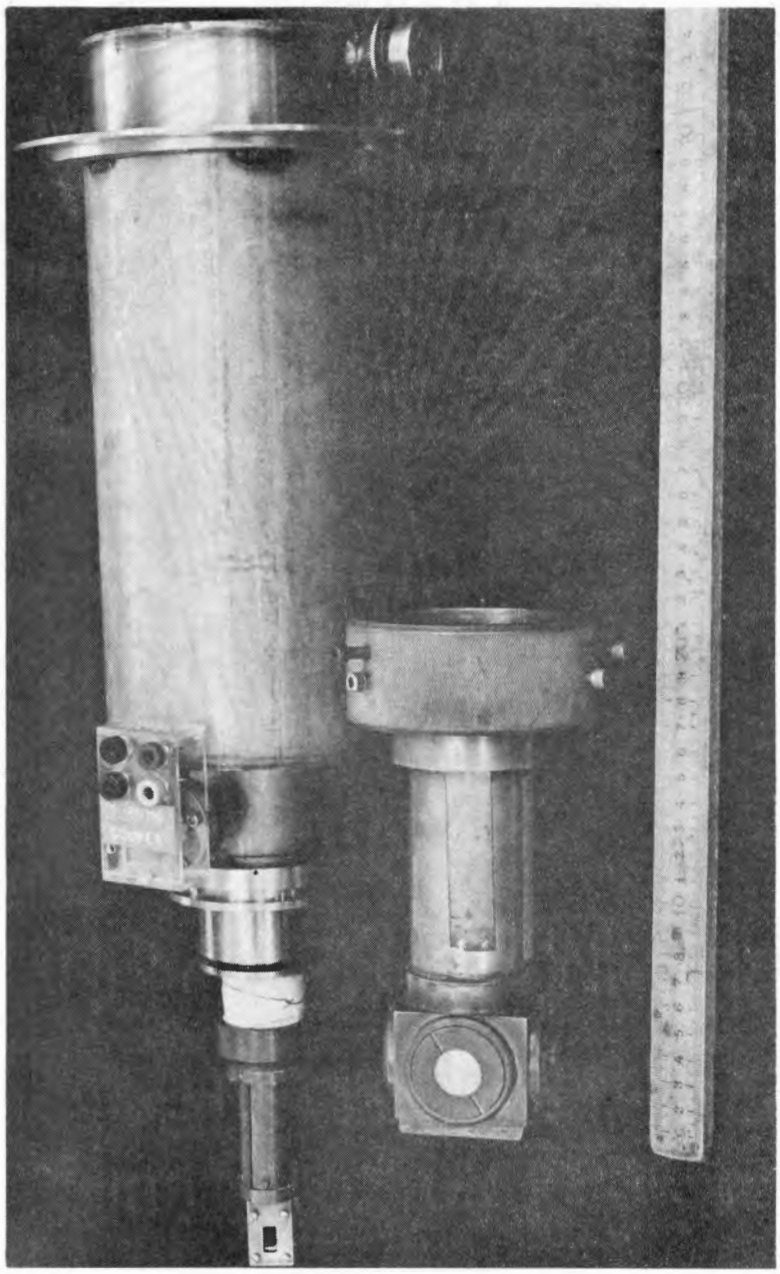

Figure 9. Photograph of TSL Cryostat

tained at room temperature.

ESR Apparatus

The ESR spectrometer used is a Varian V-4502 with an X-band (9.105 GHz) homodyne microwave bridge and a 12-inch Fieldial-regulated Varian magnet. The magnetic field modulation frequency was 100 KHz. A Varian V-4531 rectangular cavity operated in the TE102 mode is used. Measurements are made at 77K using a quartz finger Dewar, with the sample immersed directly in the liquid nitrogen. For variable temperature measurements an Air Products Heli-Tran, Model LTD-3-110 is operated in the range from 4.2K to 77K and a Varian V-4547 variable temperature accessory is used from 85K to 300K.

TSL Experimental Procedure

The samples used in this study were obtained from Dr. Richard Powell of Oklahoma State University, being cut from a boule grown, using the Czohlraski method, by the Airtron Corporation. The boule is considered "nominally pure" having not been doped with any impurities. The growth direction was the crystallographic "a" axis.

Samples were cut using a diamond saw and measured 16.0 mm x 16.0 mm x 1.0 mm. The samples are mounted unpolished and the cryostat is evacuated to a pressure of 2.0×10^{-5} Torr using a mercury vapor diffusion pump. Liquid nitrogen is then poured into the cryogenic reservoir until the system is in thermal equilibrium. The lowest obtainable sample temperature was determined to be approximately 96K.

Irradiations are performed using electrons from a High Voltage Engineering Corporation AN2000 Van de Graaff accelerator, through the aluminum windows of the cryostat. The beam energy is 1.5 MeV and the

intensity at the sample is about 5 x 10^{12} e^-/cm^2sec. To prevent warming of the sample by the electron beam the sample is irradiated for a 50 sec interval followed by a 100 sec interval with the beam off. This is repeated for a total irradiation time of 300 sec. In some of the experiments samples are subsequently irradiated at the same temperature through the quartz window with an unfiltered mercury lamp for one hour.

Many of the experiments investigated the TSL below room temperature. A simple procedure is used to warm the sample in this temperature range. Compressed air is introduced into the cryogenic reservoir with a rubber hose, with the rate of temperature rise being controlled by manual adjustment of the flow rate. The heating rate is rather consistently maintained between experiments and can usually be fitted quite well to two straight lines showing approximately 9K/min below 200K and 4K/min above 230K, with a gentle deviation from linearity between these two temperatures. Probably the major drawback of this method is the slow heating rate as the sample temperature approached 273K.

To perform experiments in the temperature range above room temperature it is necessary to use another approach. Resistive heating, using a 135 watt cartridge heater manufactured by Hotwatt Inc. driven by a manually-controlled Variac could produce a rather linear heating rate of 9K/min over a temperature range of 110K to 340K.

ESR Experimental Procedure

Samples used in this portion of the work required a different geometry but were cut from the same boule as those used for the TSL studies. Since the growth axis of the boule was known, samples were cut measuring 2.7 mm x 2.1 mm x 1.6 mm, the longest dimension corresponding to the crystallographic "c" axis.

To irradiate the sample at 77K, it is placed in a styrofoam cup full of liquid nitrogen. The sample is irradiated through the cup side with electrons of the same energy and intensity as in the TSL experiments for 5 min. The sample is then mounted in a spring-loaded Delrin sample holder while remaining in liquid nitrogen. For measurements done at 77K the sample and holder are transferred quickly into a liquid-nitrogen-filled quartz finger Dewar which is then placed in the cavity. For variable temperature experiments the variable temperature unit is first attached to the cavity and the sample and holder are transferred to the cavity. The Heli-Tran is used to measure the ESR spectrum at temperatures between 4.2K and 77K. For isochronal anneal experiments the Varian variable temperature unit is used. All ESR spectra are obtained at 85K. The sample is heated to a fixed temperature and is kept at that temperature for 5 min then returned to 85K and the spectrum remeasured. Due to problems with frost forming on the outside of the cavity, this method can only be used to temperatures around 265K. To perform annealing experiments above 273K the sample is immersed in water of fixed temperature for 5 min, then remounted and returned to the finger Dewar to be placed in the cavity.

Some photobleaching experiments were also performed. The sample is mounted on the Delrin holder and immersed in the liquid-nitrogen-filled finger Dewar. This is placed in the cavity, which has a slotted front which can allow light to enter. An Oriel Corporation Model 6253 150W Xenon lamp in a Model 6137 housing powered by a Model 8500 arc lamp power supply is used as a light source. It is placed in the plane of the sample and 0.5m from the front of the cavity.

CHAPTER IV

EXPERIMENTAL RESULTS

1. TSL Results

Figure 10 shows the TSL of $CaWO_4$ irradiated at $96^{\circ}K$ with 1.5 MeV electrons. To avoid heating of the sample it was irradiated in 50 sec time intervals, with 100 sec intervals between irradiation, for a total irradiation time of 5 min. While warming the sample the heating rate did not deviate appreciably from linearity, being about $9^{\circ}K$/min below $230^{\circ}K$ and about $4^{\circ}K$/min above that temperature. After irradiation it was noted that the sample emitted a dim blue afterglow. The spectrum of the afterglow was identical to the corrected spectrum of the $110^{\circ}K$ glow peak, shown in Figure 11. The spectra for the other glow peaks, corrected for the changing intensity of the sample by the program in the Appendix, are shown in Figures 12-15. The spectra are not corrected for phototube response, since this is very flat in the region scanned. The monochromator response was the only other factor causing changes in the recorded spectra. Since the errors are small no correction was made.

2. ESR Results

All measurements were made with the sample oriented so the magnetic field was parallel to the c-axis. The ESR spectrum of unirradiated $CaWO_4$ measured at $77^{\circ}K$ is shown in Figure 16. Figure 17 is the spectrum

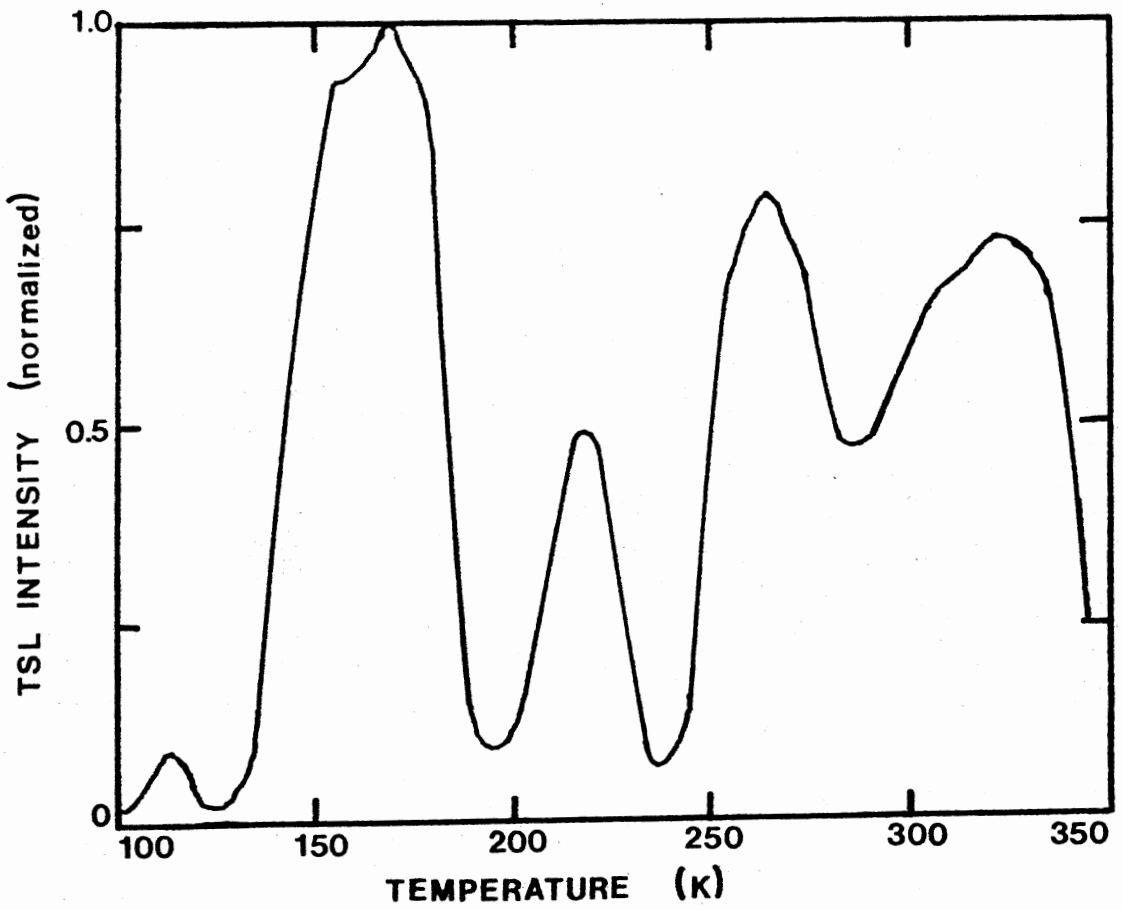

Figure 10. TSL of $CaWO_4$ Irradiated at $96^{o}K$

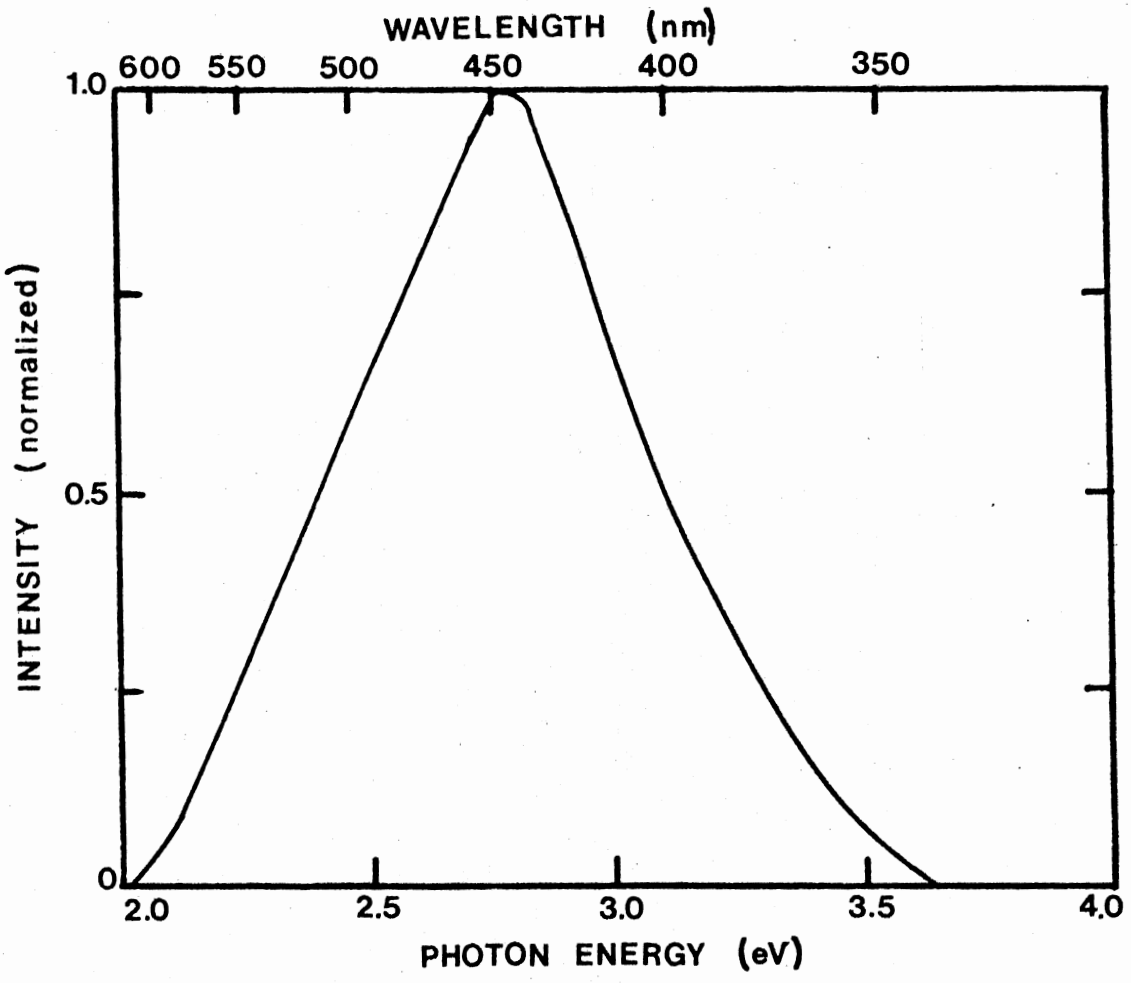

Figure 11. Spectral Output of 110 K TSL Peak

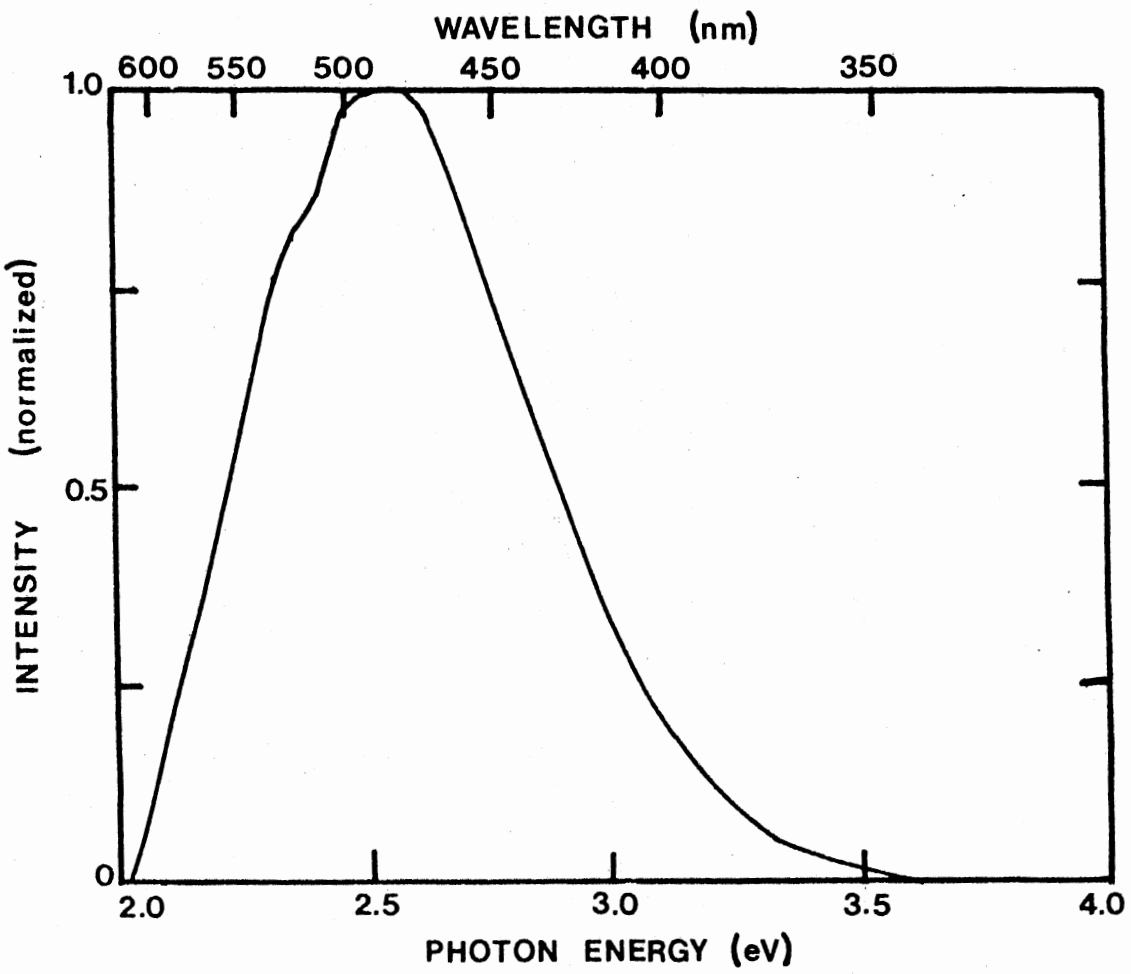

Figure 12. Spectral Output of 168 K TSL Peak

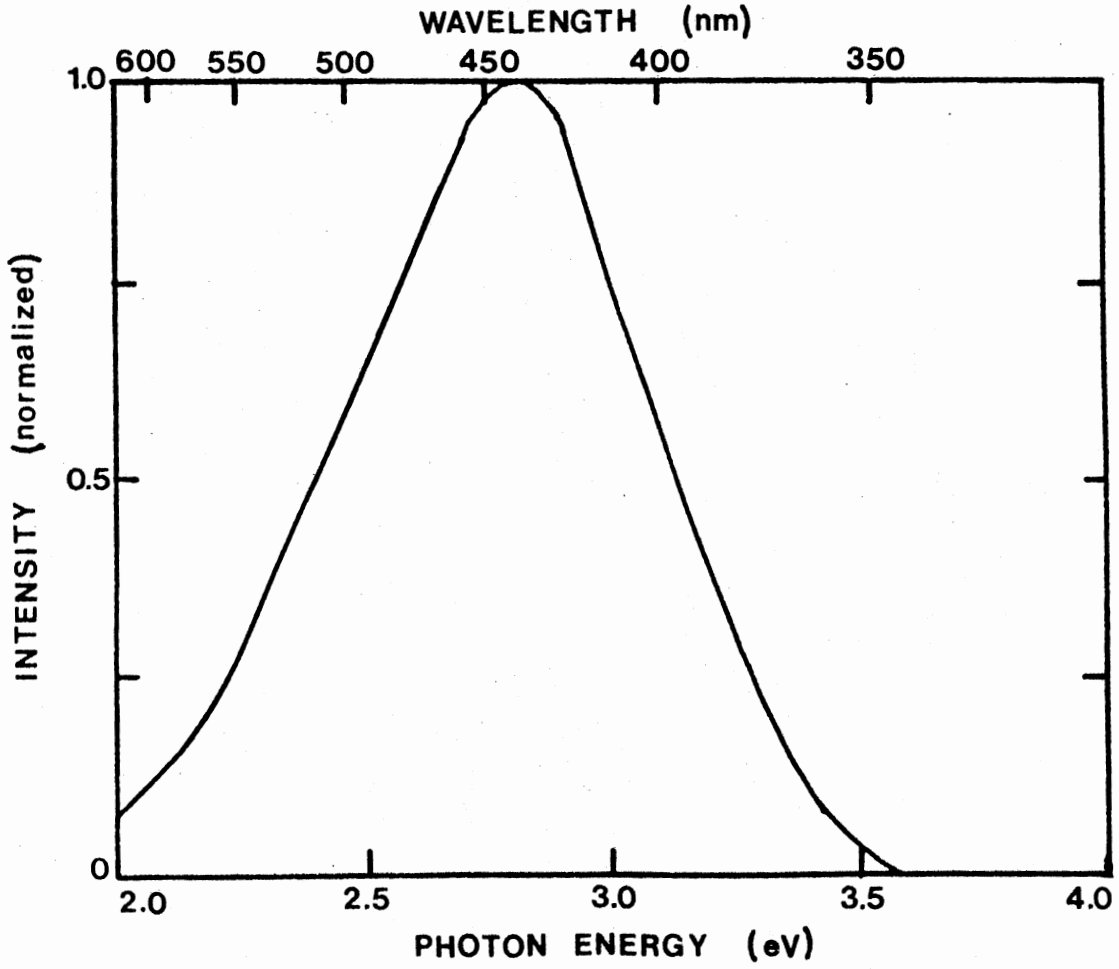

Figure 13. Spectral Output of 220°K TSL Peak

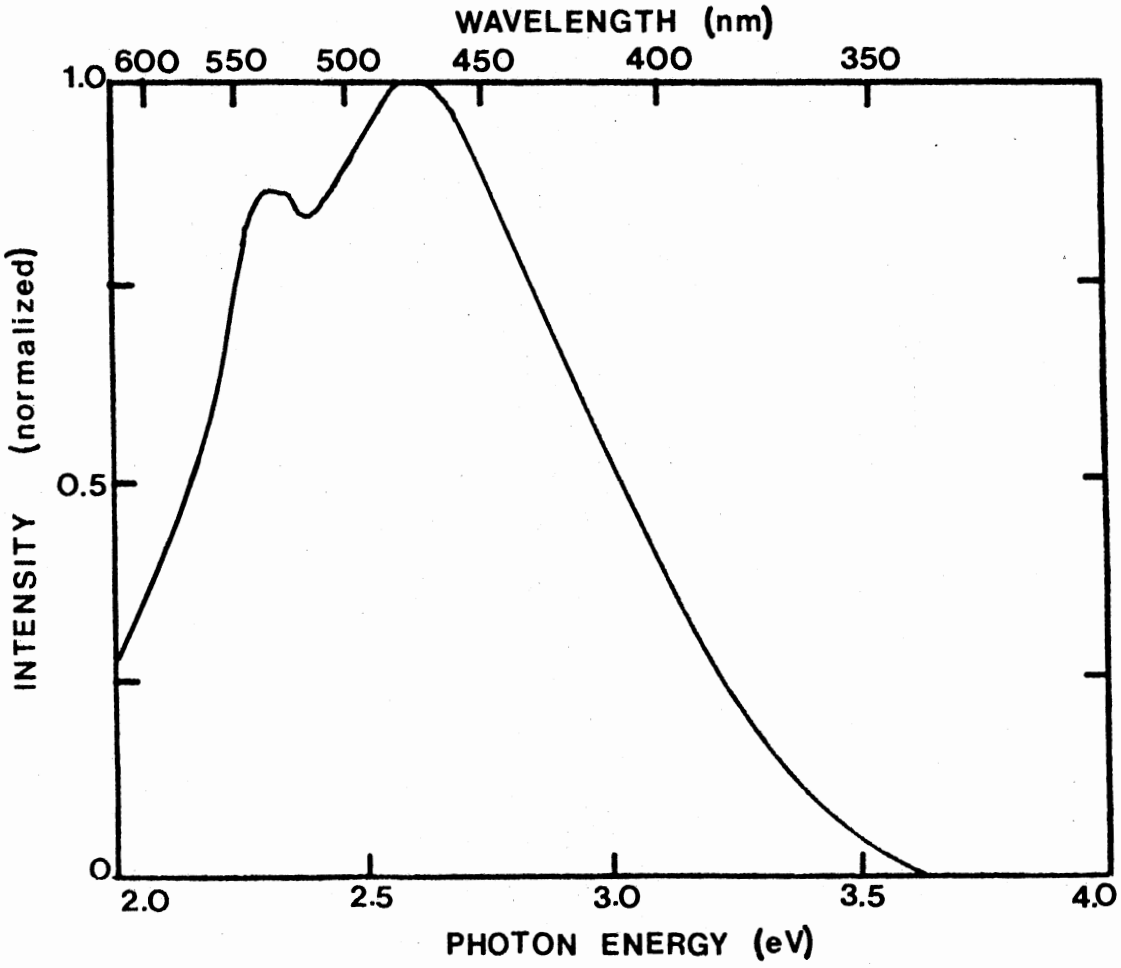

Figure 14. Spectral Output of 268°K TSL Peak

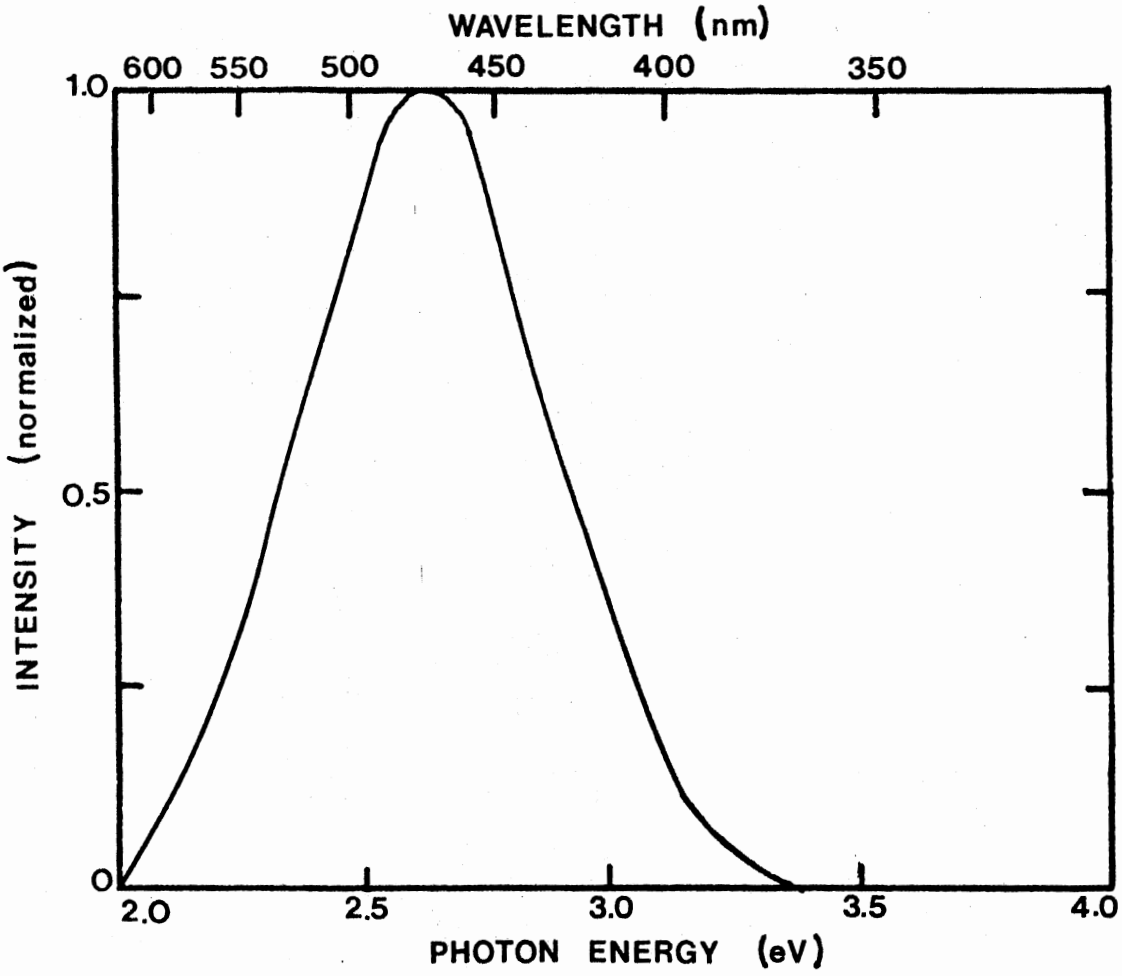

Figure 15. Spectral Output of 320 K TSL Peak

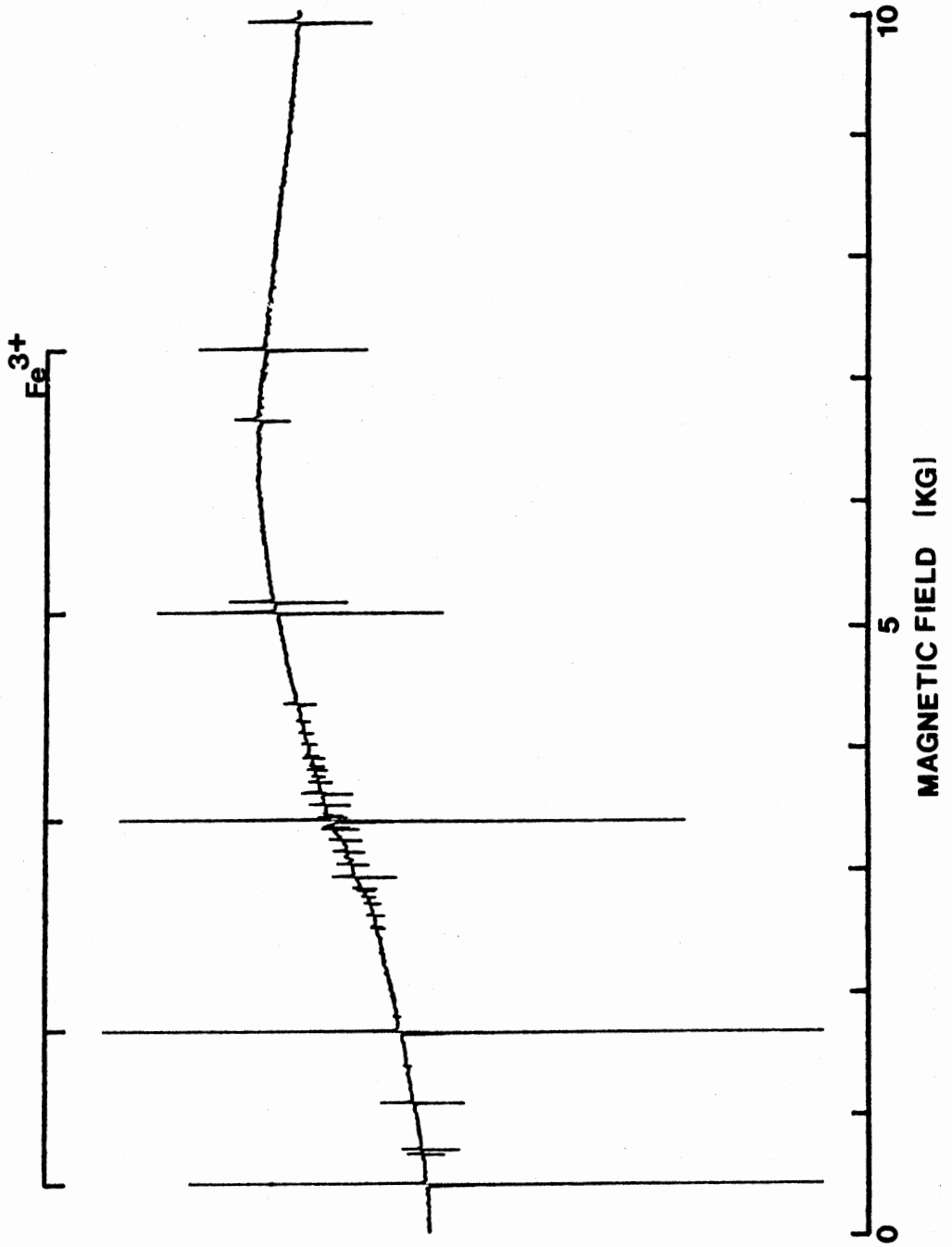

Figure 16. ESR of Unirradiated $CaWO_4$ Measured at $77^{o}K$

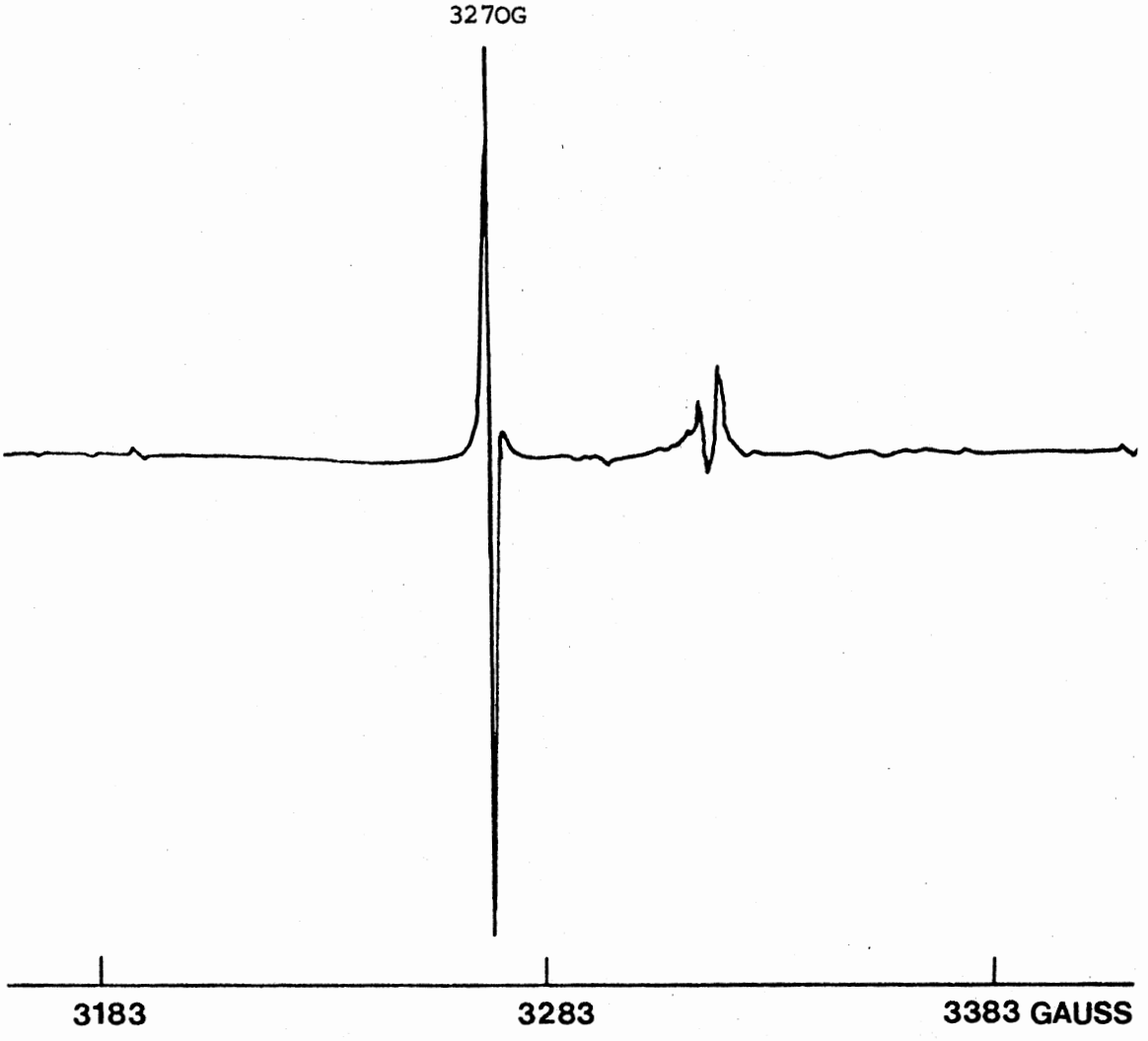

Figure 17. ESR Spectrum of Unirradiated $CaWO_4$ at $5^{o}K$

of unirradiated $CaWO_4$ measured at $5^{\circ}K$.

After a 5 min irradiation at $77^{\circ}K$ with 1.5 MeV electrons the ESR spectrum changes dramatically in the region centered at 3300G. Figure 18 shows the ESR spectrum of irradiated $CaWO_4$ measured at $77^{\circ}K$. Figure 19 shows the spectrum when measured at $5^{\circ}K$. Figure 20 is a detailed picture of the intrinsic hole center, measured at $5^{\circ}K$. Figure 21 is the ESR spectrum of $CaWO_4$ which has been irradiated at $77^{\circ}K$, warmed to room temperature briefly, then recooled to $5^{\circ}K$ and measured in the region centered at 3300G.

Figure 22 shows the isochronal anneal data for $CaWO_4$ irradiated at $77^{\circ}K$. The procedure is described in Chapter III. The TSL of $CaWO_4$ which was irradiated with 1.5 MeV electrons, in the usual manner, and then irradiated for 1 min with light from a 150W Xenon lamp positioned 0.5m from the sample is presented in Figure 23. In a related experiment the same lamp was positioned 0.5m away from the microwave cavity, which had a slotted front to admit light. In the cavity was a sample of $CaWO_4$, irradiated at $77^{\circ}K$ with 1.5 MeV electrons. The sample was irradiated at 1 min intervals, with a spectrum of the region centered at 3250G taken after each irradiation. This was done three times. The peak-to-peak amplitudes of the various paramagnetic centers measured in this region are presented in Figure 24.

Figure 25 shows the TSL of $CaWO_4$ irradiated for 1 hour at $96^{\circ}K$ with an unfiltered mercury lamp positioned 4 cm from the sample.

Analysis of these results, and a model which is formulated from them, appears in Chapter V.

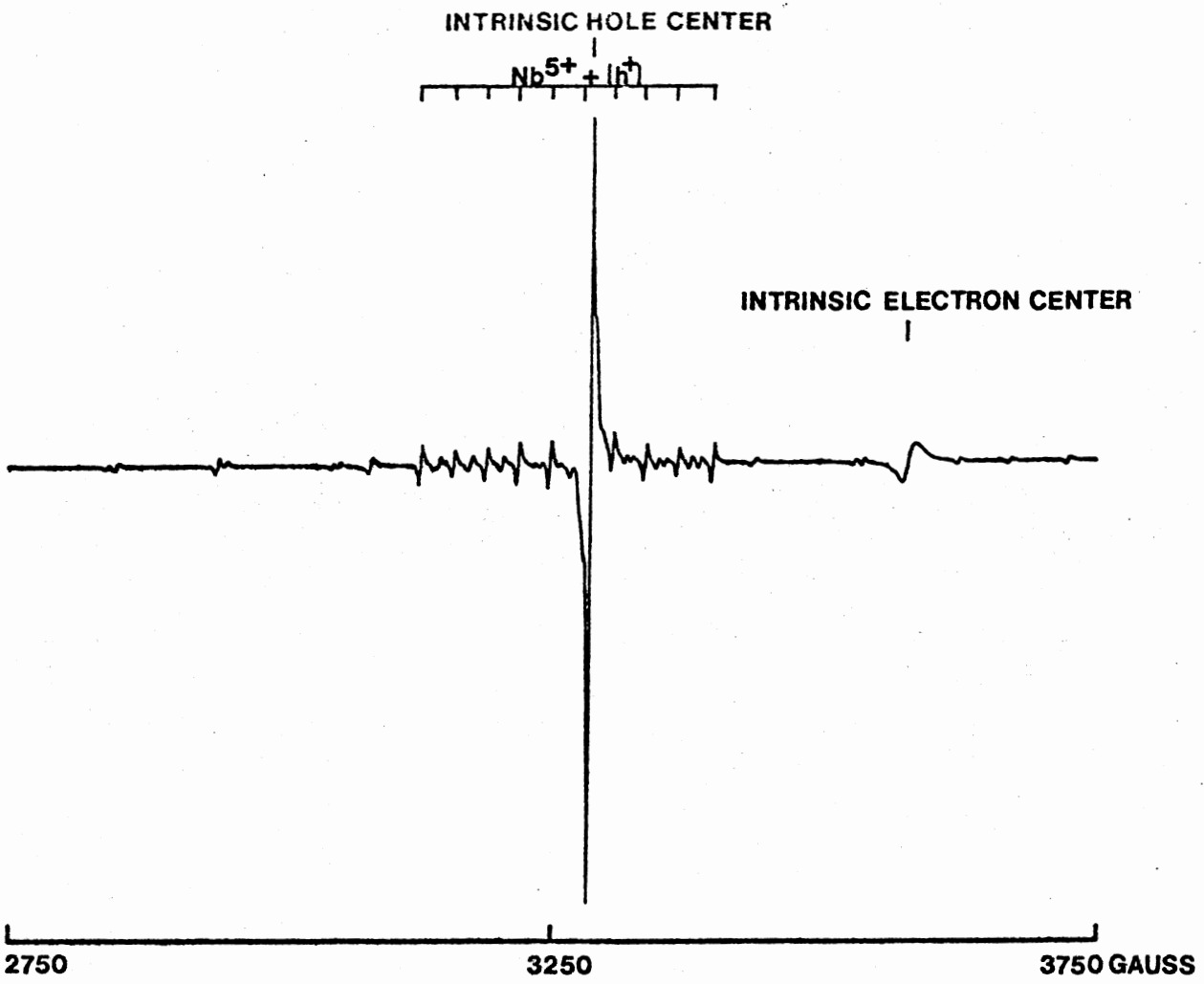

Figure 18. ESR of Irradiated $CaWO_4$ Measured at $77^{o}K$

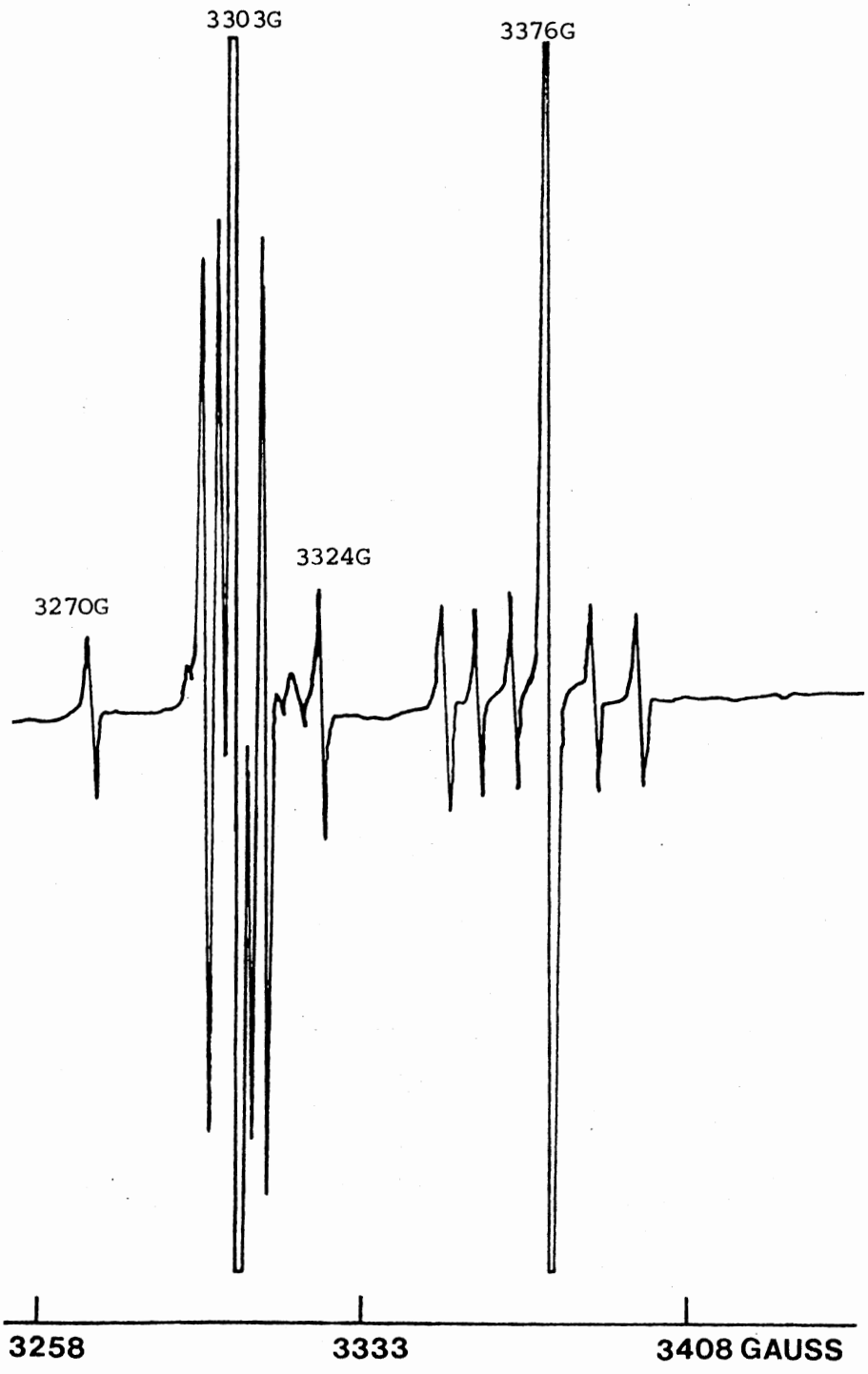

Figure 19. ESR Spectrum of $CaWO_4$ Irradiated at $77^{\circ}K$ and Measured at $5^{\circ}K$

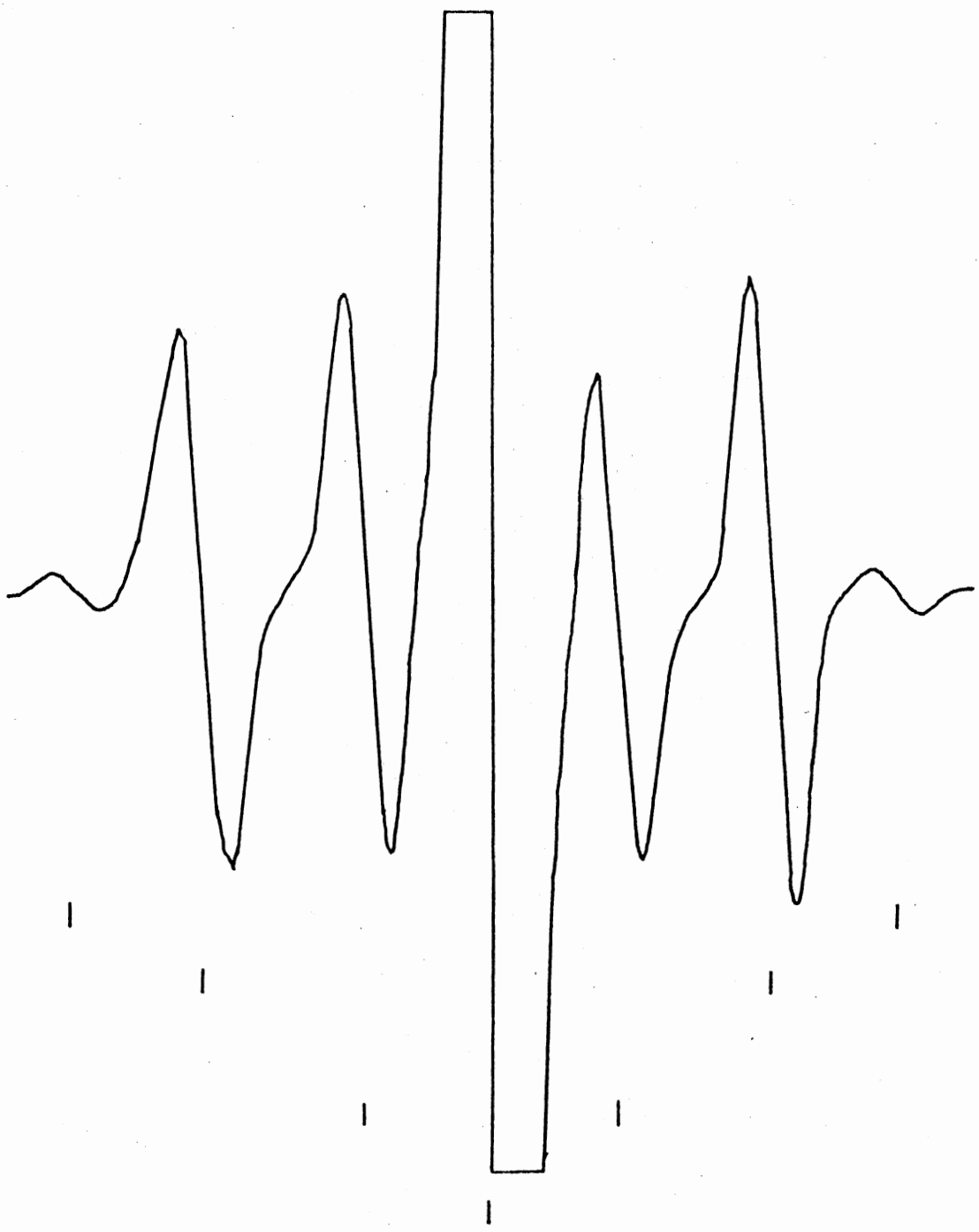

Figure 20. ESR Spectrum of Hole-Center in $CaWO_4$

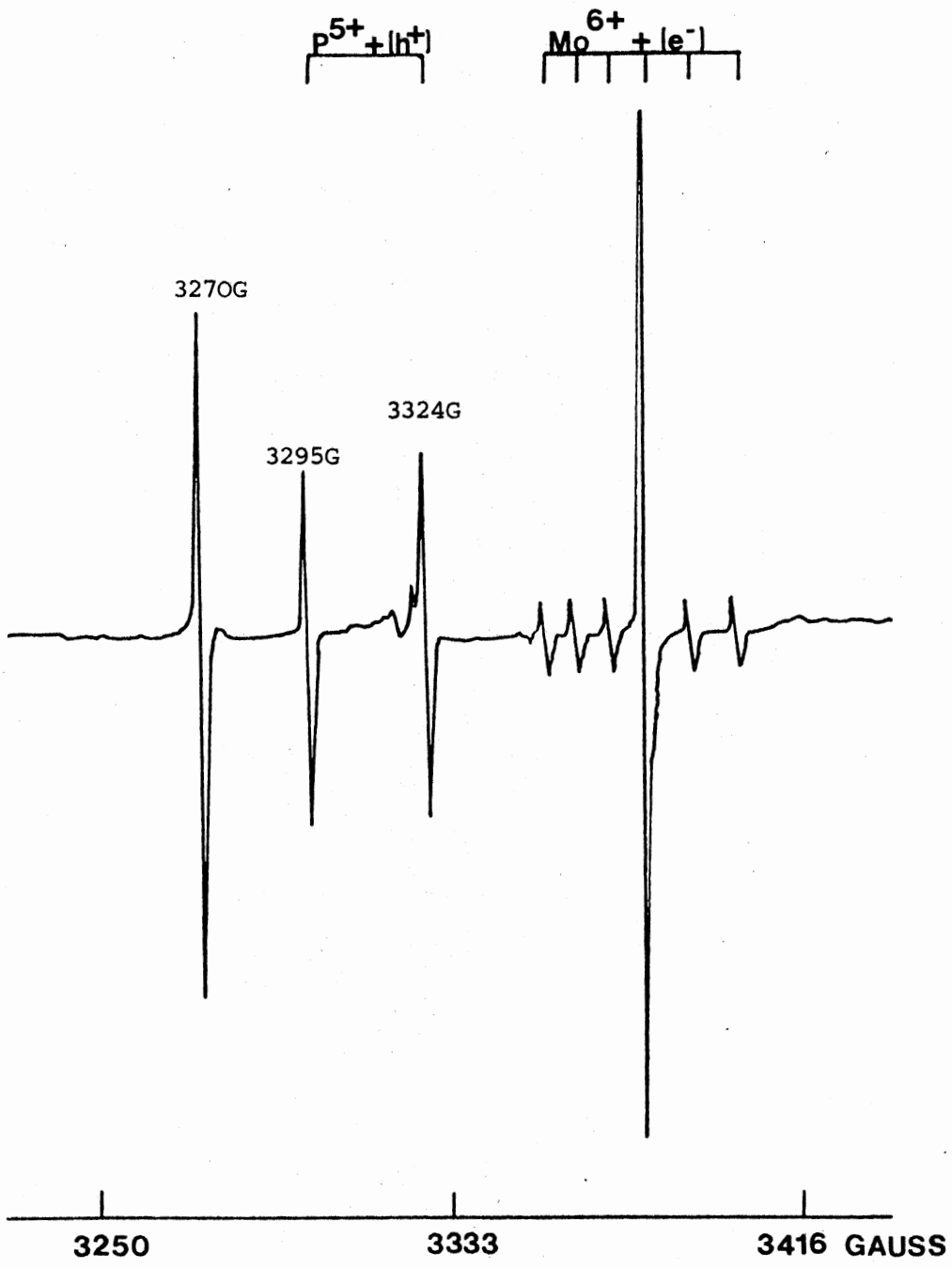

Figure 21. ESR Spectrum of $CaWO_4$ Irradiated at 77°K, Warmed to 298°K, and Measured at 5°K

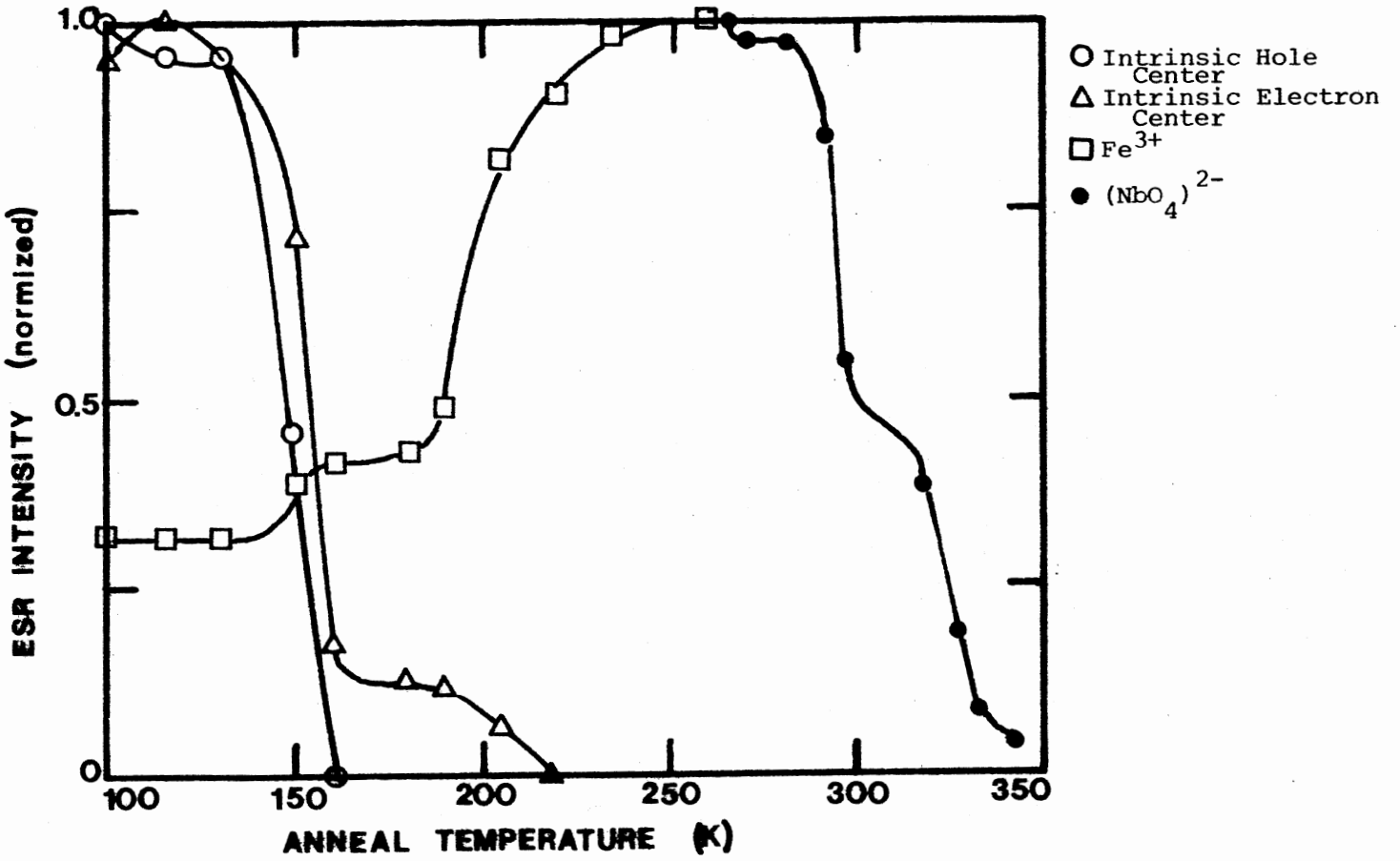

Figure 22. Isochronal Anneal of $CaWO_4$

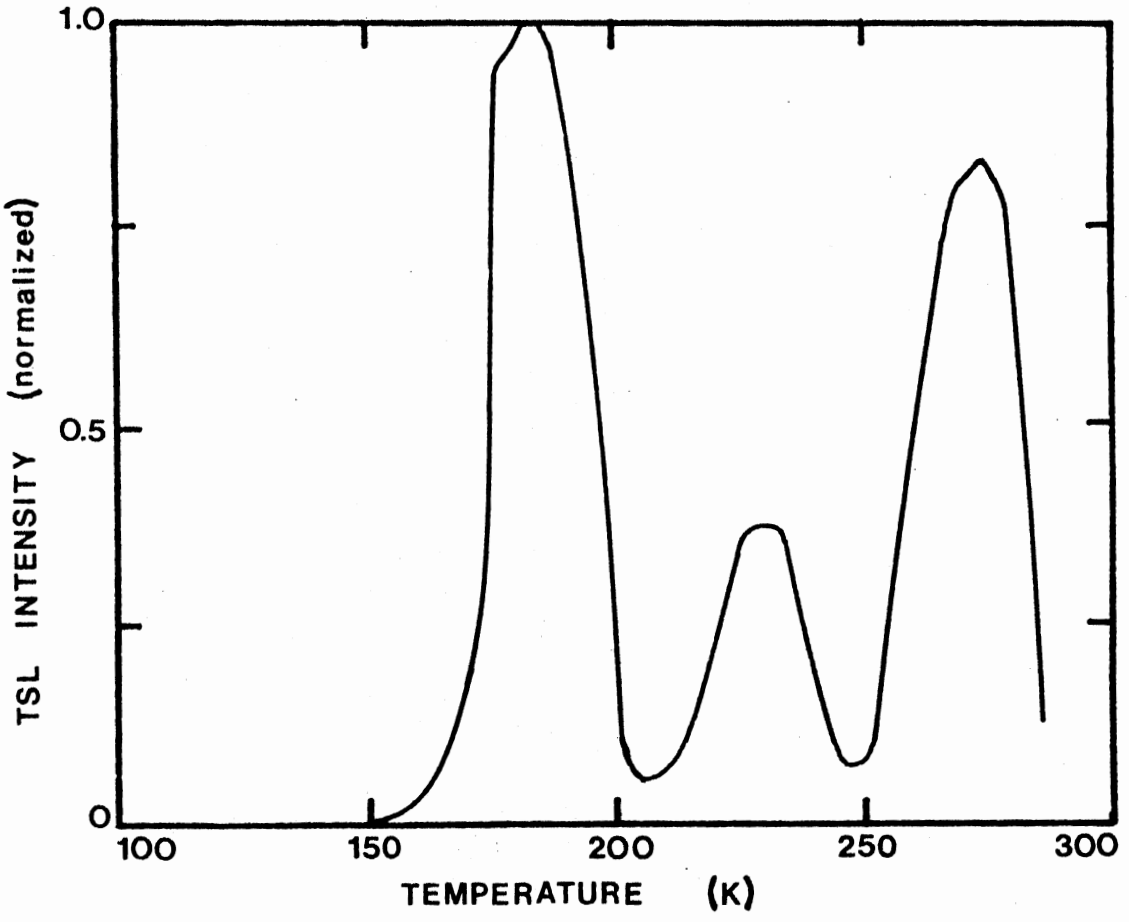

Figure 23. TSL of $CaWO_4$ Bleached With U.V. Light

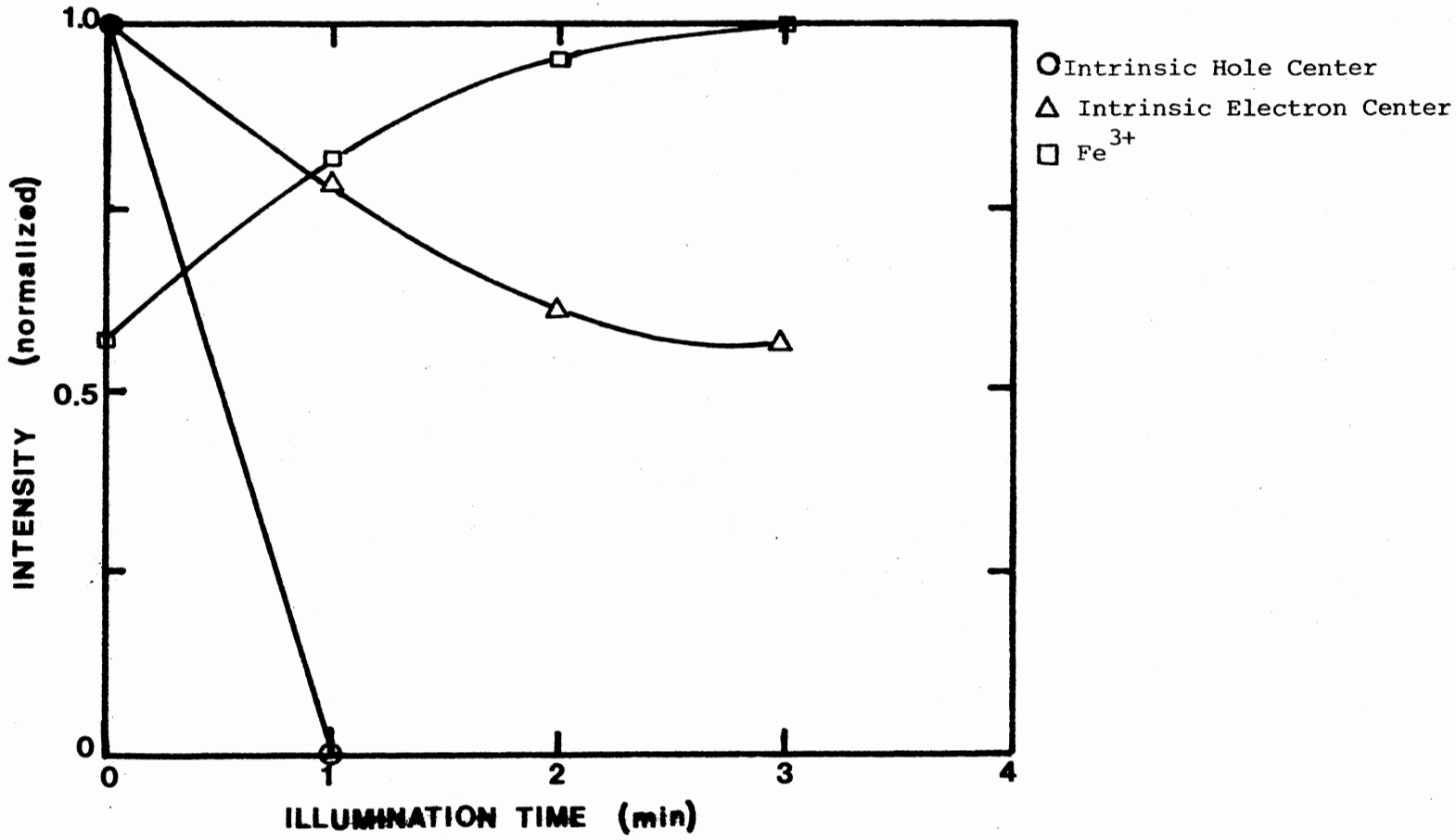

Figure 24. Change in Peak-to-Peak Amplitude of ESR Spectrum After Illumination With U.V. Light

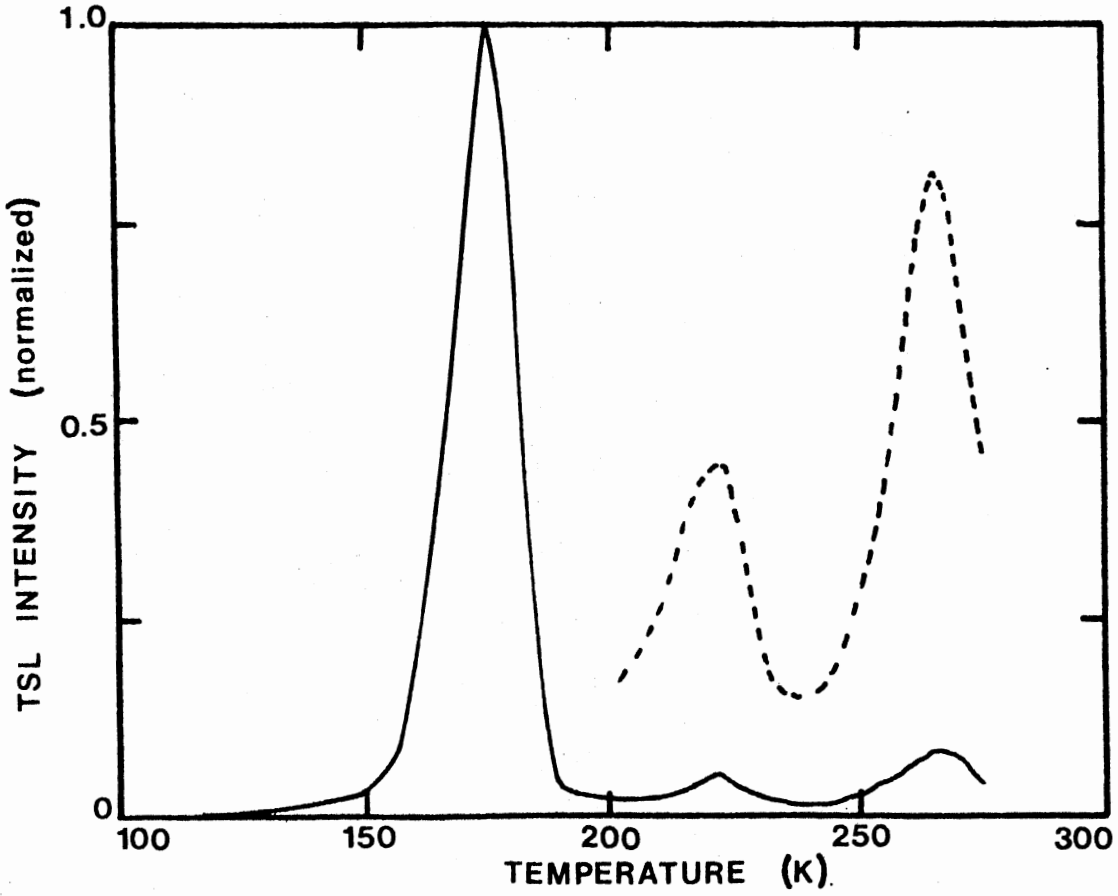

Figure 25. TSL of $CaWO_4$ Irradiated With U.V. Light (Dotted Line Indicates X10 Magnification of Intensity)

CHAPTER V

DISCUSSION

1. Analysis of ESR Spectra

When measured at 77°K, the ESR spectrum for unirradiated $CaWO_4$, shown in Figure 16, consists of six prominant lines and a large number of smaller lines, grouped near 3200G. The smaller resonances are grouped into five overlapping sets of six lines each. Such a spectrum is attributed to $^{55}Mn^{2+}$ ($S = \frac{5}{2}$, $I = \frac{5}{2}$, 100% abundant) substituting for Ca^{2+} (13). The six prominant lines all have a symmetrically spaced pair of hyperfine lines about them. This spectrum is interpreted as being due to a $S = \frac{5}{2}$ spin system, with the lower field set of five lines attributed to the allowed transitions and the high-field line being due to a forbidden transition. The most probable ion responsible for this spectrum is Fe^{3+}. This assignment was made primarily on the basis of the magnitude and intensity of the hyperfine splitting, which is characteristic of ^{57}Fe ($I = \frac{1}{2}$, 2.19% abundant). A nearly identical ESR spectrum, attributed to Fe^{3+} has been found in scheelite-structured $LiYF_4$ by Renfro et al. (14). There are two possible cation sites for this ion to substitute in, Ca^{2+} (ionic radius = 0.99Å) and W^{6+} (ionic radius = 0.68Å), Fe^{3+} (ionic radius = 0.614Å) should substitute more easily for Ca^{2+}, since less charge compensation is required.

When the temperature is lowered to 5°K the only new feature in the ESR spectrum is a sharp line at 3270G, as shown in Figure 17. At

this time insufficient data exist to make a definite statement on its identity. The lines to the right of this resonance are due to a Fe^{3+} resonance which is badly saturated.

Irradiation of $CaWO_4$ at $77^{o}K$ in the manner described in Section 4, Chapter III, results in the ESR spectrum shown in Figure 18. All the major changes occur in this region, centered at 3325G. Elsewhere the only change noted is a reduction in the signal due to Fe^{3+}. This is interpreted as resulting from a change in valence from Fe^{3+} to Fe^{2+}, making the iron ion an electron trap. The large resonance at 3285G is due to a hole while the broad resonance at 3580G is due to a trapped electron. These assignments are made based on the shift away from the free-electron g-value (positive for a hole, negative for an electron) and their stability of position as the orientation of the magnetic field was changed from being parallel to the c axis to some arbitrary orientation. The lines on either side of the hole signal may be seen to consist of ten resonances (one of which is masked by the hole signal) plus a series of smaller lines in between. The ten lines arise from the hyperfine interaction of a $I = \frac{9}{2}$, 100% abundant nucleus with a $S = \frac{1}{2}$, I = 0 hole, while the smaller resonances are probably due to forbidden transitions. A Nb^{5+} ion ($I = \frac{9}{2}$, 100% abundant) which substitutes for W^{6+} and has trapped a hole on an adjacent oxygen forming $(NbO_4)^{2-}$, will produce such a spectrum.

When $CaWO_4$ irradiated at $77^{o}K$ is measured at $5^{o}K$, the spectrum shown in Figure 19 results. The 3270G signal due to the unknown paramagnetic center has been reduced, indicating change to a nonparamagnetic state. The five-line resonance centered at 3303G is shown in detail in Figure 20. The center line is due to the $S = \frac{1}{2}$ hole. The two pairs of

superhyperfine lines symmetrically spaced around the center line are due to interactions with two nonequivalently situated ^{183}W nuclei ($I = \frac{1}{2}$, 14.4% abundant). The outer pair of lines occur because the ^{183}W nucleus is part of the $(WO_4)^{2-}$ complex where the hole is trapped. The inner pair of lines occurs when the ^{183}W nucleus is part of the $(WO_4)^{2-}$ complex adjacent to the complex trapping the hole. The outermost pair of lines is the superhyperfine interaction of a ^{183}W nucleus on an adjacent ^{183}W nucleus. Thus, this unequal splitting of the superhyperfine interactions indicates that at $5^{o}K$ the hole is primarily trapped on one $(WO_4)^{2-}$ complex. This conclusion is consistent with the conclusion reached by Biederbick et al. (7). At $77^{o}K$ this hyperfine interaction is only partially resolved, according to Born et al. (5), leading them to the conclusion that at $77^{o}K$ the hole is equally shared between two $(WO_4)^{2-}$ tetrahedra. Presumably this sharing is actually between two equivalent oxygen ligands. We were unable to confirm this conclusion since, above $30^{o}K$, the spin-lattice relaxation time becomes such that the niobium hyperfine interaction is no longer saturated and becomes measurable, masking the hole center's hyperfine interactions.

Returning to Figure 19, at 3376G there is a strong resonance with six hyperfine lines, one of these being masked by the large line so that only five hyperfine lines appear. This spectrum is due to a substitutional Mo^{6+} trapping an electron to become Mo^{5+}. The hyperfine spectrum is characteristic of molybdenum ($I = \frac{5}{2}$; ^{95}Mo 15.72% abundant ^{97}Mo 9.46% abundant).

The resonance at 3324G can be attributed to a specific paramagnetic center by analyzing what happens when the sample is warmed to room temperature and then recooled to $5^{o}K$. The spectrum which results

is shown in Figure 21. The unknown paramagnetic center has increased in concentration and the $(MoO_4)^{3-}$ complex concentration has decreased. Of particular interest are the two lines at 3295G and 3324G. This spectrum is characteristic of ^{31}P ($I = \frac{1}{2}$, 100% abundant) at a tungsten site which has trapped a hole to form a $(PO_4)^{2-}$ complex. The molybdenum and phosphorus centers have been reported earlier, by Hofstaetter et al. (15).

It was found that the Mn^{2+} signals reported earlier do not change after irradiation and thus do not act as traps for electrons or holes. The electron center mentioned earlier had no hyperfine interactions which were detectable and thus the site where it is trapped was not determined. Evidently, however, it is the same center reported by Zeldes and Livingston (4) and is due to electrons trapped at tungstate complexes, forming $(WO_4)^{3-}$, which are stabilized by a neighboring defect.

The concentration of some of the paramagnetic centers was measured to within an accuracy of 25% using an Al_2O_3 crystal with a known number of Cr^{3+} ions as a standard. The centers analyzed were the intrinsic hole center, the electron center, the Fe^{3+} ion, and the hole associated with the Nb^{5+} ion. The $Al_2O_3:Cr^{3+}$ standard was mounted next to a sample of $CaWO_4$ which had been irradiated at $77^{o}K$. The crystals were brought into the cavity without warming and the two Cr^{3+} lines, at 1800G and 5300G were measured, along with the lines of interest. Careful note was made of the modulation amplitude, signal level, sweep rate of the magnetic field, and the microwave power. The absorption was found by double integrating the first derivative measurements. This information was substituted into formula D-12, p. 462 of Wertz and Bolton's book, Electron Spin Resonance: Elementary Theory and Practical

Applications (16). The results are tabulated in Table I. One slight approximation was used. The g-factor of the paramagnetic centers was assumed equal to the g-factor of the standard, but this introduces an error of no more than one percent.

TABLE I

CONCENTRATION OF PARAMAGNETIC CENTERS IN $CaWO_4$ IRRADIATED WITH WITH 1.5 MeV ELECTRONS FOR 5 MIN AT 77°K AND MEASURED AT 77°K

Paramagnetic Center	Concentration Unpaired Spins/cm^3
Fe^{3+}	4.2×10^{16}
$(NbO_4)^{2-}$	7.4×10^{17}
Intrinsic hole center	2.7×10^{17}
Intrinsic electron center	2.0×10^{17}

Also, there is more uncertainty in the computation of the area under the absorption curve for the intrinsic hole center. This curve includes the absorption of one of the iron lines and one of the niobium hyperfine lines. Using the value of the area under the curve for a niobium hyperfine line and a properly scaled iron line the contribution from these two lines were subtracted from the total area. The corrected area was used in the calculation of the concentration. The uncertainty in doing the double integration is thus magnified for the intrinsic hole center.

2. Correlation of Isochronal Anneal Data With TSL

Isochronal anneal data, shown in Figure 22, and taken in the manner described in Section 4, Chapter III, may now be used to identify the processes responsible for TSL. The TSL data has been presented in Figure 10. Clearly the first half of the 168^{o}K glow peak is largely associated with the recombination of the intrinsic hole center with the intrinsic electron center. The two-step annealing of the intrinsic electron center is indicative of hole release and recombination at the intrinsic electron trap. For electrons to be released at two different temperature ranges would imply that the electrons are trapped at non-equivalent lattice sites. This inequivalence would be apparent upon examination of the ESR data; since it is not seen, the conclusion is that all intrinsic electron center traps are equivalent. The statement that hole release is responsible for the decay of the intrinsic electron and hole centers has been made before, by Born et al. (5). However, their conclusion was based more on their model than on supportive data.

From the isochronal anneal data it may be seen that some of the lower half of the 168^{o}K glow peak is due to the recombination of holes with electrons trapped at iron sites, changing the valence from 2+ to 3+. This additional recombination is responsible for the only partial annealing of the intrinsic electron center. The isochronal anneal data taken thus far does not identify the recombination process responsible for the upper half of the 168^{o}K peak. Some possibilities will be discussed later.

The arguments used to conclude that hole release is responsible

for the annealing of the intrinsic electron center are also valid in identifying the recombination process responsible for the 220°K glow peak. The isochronal anneal data indicates a two-step annealing of the electron trapped at the Fe^{3+} ion. Since the ESR data does not indicate two nonequivalent lattice sites for the iron ion it must be concluded that recombination occurs at the iron ion at both anneal stages. Thus, the 220°K glow peak is due to the release of a hole and its recombination with an electron trapped at a Fe^{3+} ion. The isochronal anneal data taken so far does not identify the center responsible for the released holes.

The hole trapped at the $(NbO_4)^{3-}$ complex remains stable, according to the isochronal anneal data, until 280°K. Comparing Figure 21 to Figure 19, it is clear that warming an irradiated sample of $CaWO_4$ to room temperature briefly and recooling causes a decrease in $(MoO_4)^{3-}$ concentration and an increase in $(PO_4)^{2-}$ concentration. From the isochronal anneal data the source of holes responsible for these changes is the $(NbO_4)^{2-}$ complex. At 280°K the $(NbO_4)^{2-}$ releases its hole, becoming $(NbO_4)^{3-}$. The holes are either retrapped at $(PO_4)^{3-}$ complexes or recombine with an electron at a $(MoO_4)^{3-}$ complex to produce TSL. At some higher temperature recombination of charges trapped at $(PO_4)^{2-}$ and $(MoO_4)^{3-}$ complexes occurs.

Insufficient isochronal anneal data exists at this time to identify the recombination processes responsible for the 110°K and 268°K glow peaks, or the upper half of the 168°K glow peak. Possible recombination processes responsible for these glow peaks will be discussed at the end of the chapter.

3. Analysis of Photobleaching Data

The TSL of $CaWO_4$ irradiated with high energy electrons at 96°K and then bleached for 1 min with ultraviolet light is shown in Figure 23. The change in the peak-to-peak amplitude of the intrinsic electron and hole centers, and the Fe^{3+} ion are shown in Figure 24. This behavior has been reported by Zeldes and Livingston (4).

The ESR data may be used to explain the TSL. After a 1 min illumination, the intrinsic hole center has been bleached out completely, and cannot provide holes to recombine at electron traps. Hence, one would expect no TSL where the lower half of the 168°K glow peak is and Figure 23 confirms this. Presumably the illumination produces free electron-hole pairs, with the electrons recombining at the intrinsic hole center and holes at the intrinsic electron center and Fe^{2+} ion. Since the concentration of Fe^{2+} has decreased, the TSL from the 220°K glow peak should also be less. Comparison of Figure 24 with Figure 10 confirms this. The ability to predict the observed TSL, using the model proposed in the last section to interpret the ESR data, supports the model's validity.

4. Analysis of Observed Luminescence

One of the most difficult pieces of data to understand is the luminescence spectrum for the 168°K and 268°K glow peaks. The TSL is composed of two components, with maxima at 440 nm and 520 nm. Before this study no one had reported TSL with a green emission in nominally pure $CaWO_4$.

Our samples were obtained from Dr. Richard Powell, who had purchased them in order to do energy transfer studies. His group found that exci-

tation into the strong absorption region in $CaWO_4$ produced 440 nm luminescence while excitation into the weak absorption region produced 520 nm luminescence (17). Their interpretation at that time was that this 520 nm luminescence was due to transitions in the $(WO_4)^{2-}$ complex which do not normally occur. These transitions occur because of nearby chemical or structural defects which perturb the local symmetry and crystal field strength. Since then other researchers have made similar observations (18). Recently, work on the luminescence of tungstates and molybdates has been done by a group headed by Dr. G. Blasse at Utrecht. They have also observed this green luminescence and attribute it to transitions in a WO_3 complex, i.e., a $(WO_4)^{2-}$ complex with an oxygen vacancy (19,20).

If this interpretation is correct, then one would reasonably expect that green luminescence should be observed for the other glow peaks as well. The fact that it is not observed makes this interpretation suspect as an explanation for the observed TSL.

An alternative explanation is that the luminescence is due to an impurity. Mikhalev et al. (21) found that doping $CaWO_4$ with phosphorus produces a TSL peak at 263°K and changes the spectral maximum of a 295°K TSL peak to 510-530 nm. The report of a TSL peak at 263°K when $CaWO_4$ is doped with phosphorus agrees well with the presence of phosphorus and a 268°K TSL peak in our sample. It is proposed that electrons recombining at $(PO_4)^{2-}$ sites is the mechanism responsible for both the upper half of the 168°K TSL peak and the 268°K peak, with spectral maxima at 520 nm. More data must be taken to confirm this hypothesis, however.

As was mentioned in the Introduction, Kröger (2) concluded that the 440 nm luminescence from u.v.-irradiated $CaWO_4$ is due to transitions

in the $(WO_4)^{2-}$ complex. The TSL in the lower half of the 168°K peak has a spectral maximum at 440 nm. Our model proposes as the cause of this portion of the glow peak recombination of a hole at the "intrinsic electron trap" which according to Zeldes and Livingstone (4) is a perturbed $(WO_4)^{3-}$ complex. Hence, the model predicts the color of the luminescence. The 220°K peak also luminesces at approximately 440 nm. Our model proposes the recombination of holes at Fe^{2+} ions as the cause of this glow peak. A blue emission as Fe^{2+} changes to Fe^{3+} has been found in MgO by Sibley et al. (22). Thus, for this TSL peak the model is not necessarily in disagreement with the data. The upper half of the 168°K peak also shows 440 nm luminescence. It is tempting to associate this, too, with transitions in $(WO_4)^{2-}$ complexes, but as yet no satisfactory recombination mechanism is evident from isochronal anneal data. The luminescence from the 320°K TSL peak also has a maximum at about 440 nm. Our model proposes the recombination of holes at $(MoO_4)^{3-}$ complexes to be responsible for the luminescence. While pure $CaMoO_4$ luminesces in the green (19), the low concentration (no more than several hundred ppm) would not affect the tungstate-configuration crystal field appreciably and the resulting distorted molybdate crystal field could be responsible for the shift in emission maximum.

5. Analysis of TSL From U.V.-Irradiated $CaWO_4$

The TSL of $CaWO_4$ irradiated for one hour at 96°K with light from an unfiltered mercury lamp is shown in Figure 25. This sample had no prior history of irradiation. The observed TSL can be qualitatively explained by our model. Ultraviolet light creates electron-hole pairs resulting in charges trapped at electron and hole traps associated with

impurities. The intrinsic traps associated with electron irradiation are bleached as fast as they are created. This is why the data looks so much like the TSL of photobleached $CaWO_4$, shown in Figure 23. Both experiments lead us to propose that the 110°K TSL peak may also be due to intrinsic lattice defects. This proposal is, at the moment, extremely speculative and more data is needed to verify it.

6. Summary

The use of TSL and EPR has made it possible to identify the radiation-induced defects in electron-irradiated, nominally pure $CaWO_4$. The defects were found to be both intrinsic to the lattice and associated with impurities. By using isochronal anneal and photobleaching data, along with observation of the spectral composition of the TSL, a model which associates particular recombination processes with the observed TSL has been proposed.

It was found that TSL peaks are produced when $CaWO_4$ is irradiated with 1.5 MeV electrons at 96°K and subsequently warmed to 350°K. The TSL peak temperatures occur at 110°K, 168°K, 220°K, 268°K, and 320°K. The luminescence from these glow peaks is broad and has a maximum at 440 nm. An additional, overlapping band at 520 nm is emitted by the 168°K and 268°K glow peaks.

ESR studies indicate that Mn^{2+}, Fe^{3+}, P^{5+}, Nb^{5+}, and Mo^{6+} exist as impurities in the $CaWO_4$ samples before irradiation. The concentration of impurities was about 100 ppm. The iron and manganese substitute for calcium and the phosphorus, niobium, and molybdenum substitute for tungsten. During irradiation with 1.5 MeV electrons at 77°K the iron and molybdate complex trap electrons and the phosphate and niobate com-

plexes trap holes. Irradiation also produces hole and electron traps which are intrinsic to the lattice. At $5^{o}K$ the hole is trapped on or near a $(WO_4)^{2-}$ complex and interacts strongly with an adjacent $(WO_4)^{2-}$ complex. Studies on the electron trap are not conclusive, but are consistent with the previous work of Zeldes and Livingstone (4), who believe the electron trap is a $(WO_4)^{3-}$ complex stabilized by a nearby defect.

The data taken so far supports the following conclusions: The $168^{o}K$ glow peak is due in part to the release of holes from the intrinsic hole trap and their recombination at the intrinsic electron trap and the iron ion. The $220^{o}K$ glow peak is due to the recombination of holes with electrons trapped at iron ions. The $320^{o}K$ glow peak is due to the recombination of holes released from niobate and phosphate complexes with electrons trapped at molybdate complexes.

It is tentatively suggested that the $110^{o}K$ glow peak is also due to electrons and holes trapped at intrinsic lattice defects. Part of the $168^{o}K$ glow peak and the $268^{o}K$ glow peak are due to the recombination of electrons with holes trapped at phosphate complexes. It is this recombination which is responsible for the 520 nm luminescence.

7. Suggestions for Further Studies

Several questions remain unanswered, after the data taken was analyzed. One of these questions concerns the exact nature of the intrinsic hole center. Is it a V_k type center as proposed by Born et al. (5), or is it trapped on only one tungstate complex and simply interacts with a nearby tungstate complex (7). It has been stated that self-trapped holes do not occur in the oxide materials (23). However, this

may be the case in the more complicated oxides like $CaWO_4$. To check this, a study of the superhyperfine splitting should be conducted at temperatures above 5K. If the intrinsic hole center is truly a self-trapped hole then as the temperature is raised the splitting will become more equal as the hole is shared more equally between the two tungstate tetrahedra. An additional check on the nature of the intrinsic hole center would be to look for O^{17} hyperfine interactions. The natural abundance of O^{17} is very low, only 0.037%, but the signal-to-noise ratio is very good at $5^{o}K$ and it may be possible to detect the interaction. This would help precisely determine the intrinsic hole center's location. If the interaction is too weak to be detected then growing crystals which are enriched with O^{17} may give a detectable interaction.

To verify some of the proposed recombination processes it will be necessary to do isochronal anneal studies on the paramagnetic molybdate and phosphate complexes. The identity and isochronal anneal data on the unknown paramagnetic center must also be established. This type of signal may be due to a rare earth impurity, and if it is such an impurity, may be the cause of a low intensity, very sharp luminescence at 313 nm. This luminescence is associated with the $168^{o}K$ peak, and to date is not identified with any paramagnetic center.

Finally, a careful ESR study of the Fe^{3+} ion in $CaWO_4$ should be conducted. The spectrum should be measured at 20GHz, to improve resolution and, hopefully, eliminate the forbidden transitions. The angular dependence of the lines should be done at 9.1 GHz, to determine the precise site symmetry. At this time only one report on the ESR spectrum of Fe^{3+} in $CaWO_4$ exists (24), and the authors go to great lengths to explain their four line spectra. Since there are discrepancies between our findings and theirs, another look at iron in $CaWO_4$ is in order.

REFERENCES

1. Zalkin, A. and D. H. Templeton, J. Chem. Phys. 40, 501 (1964).

2. Kröger, F. A. Some Aspects of the Luminescence of Solids, Elsevier Publishing Co., Inc. (1948).

3. Sayer, M. and A. D. Souder, Can. J. Phys. 47, 463 (1969).

4. Zeldes, H. and R. Livingston, J. Chem. Phys. 34, 247 (1961).

5. Born, G. K., R. J. Grasser, and A. O. Scharmann, Phys. Status Solidi 28, 583 (1968).

6. Born, G., A. Hofstaetter, A. Scharmann, and G. Schwartz, J. Lumin. 42, 641 (1970).

7. Biederbick, R., G. Born, A. Hofstaetter, and A. Scharmann, Phys. Status Solidi B 69, 55 (1975).

8. Koehler, H. A. and C. Kikuchi, Phys. Status Solidi B 43, 423 (1971).

9. Randall, J. T. and M. H. F. Wilkins, Proc. Roy. Soc. A, 184, 366 (1945).

10. Garlick, G. F. J. and A. F. Gibson, Proc. Roy. Soc. A, 60, 574 (1948).

11. Kelly, P., M. J. Laubitz, and P. Bräunlich, Phys. Rev. B, 4, No. 6, 1960 (1971).

12. Stout, D. F. Handbook of Operational Amplifier Circuit Design Chapter 10, pp. 8-12 (McGraw-Hill, 1976).

13. Chu, K. C. and C. Kikuchi, Phys. Rev. 169 752 (1968).

14. Renfro, G. M., L. E. Halliburton, W. A. Sibley, and R. F. Belt, J. Phys. C 13, 1941 (1980).

15. Hofstaetter, A., J. Planz, and A. Scharmann, Z. Naturforsch 32a, 957 (1977).

16. Wertz, J. E. and J. R. Bolton, Electron Spin Resonance: Elementary Theory and Practical Applications (McGraw-Hill, 1972).

17. Treadaway, M. J., and R. C. Powell, J. Chem. Phys. 61, 4003 (1974).

18. Grasser, R. and A. Scharmann, J. Lumin 12, 473 (1976).

19. Groenink, J. A., C. Hakfoort, and G. Blasse, Phys. Status Solidi A 54, 329 (1979).

20. Groenink, J. A., and G. Blasse, J. Solid State Chem. 32, 9 (1980).

21. Mikhalev, A. A., B. N. Meleshkin, I. G. Kaplenov, and L. P. Podsadnyaya, Izv. Akad. Nauk SSSR Ser. Fiz. 38, 1151 (1974).

22. Sibley, W. A., J. L. Kolopus, and W. C. Mallard, Phys. Status Solidi 31, 223 (1969).

23. Henderson, B. and J. E. Wertz, Defects in the Alkaline Earth Oxides, p. 56 (Halsted Press, New York - 1977).

24. Kedzie, R. W., D. H. Lyons, and M. Kestigian, Phys. Rev. 138, 918 (1965).

APPENDIX

FORTRAN SOURCE CODE FOR SPECTRUM CORRECTING

PROGRAM TLSPEC

```
C   THIS PROGRAM CORRECTS THE SPECTRUM OF A THERMOLUMINESCING SAMPLE.
C   DUE TO THE CHANGING INTENSITY OF THE SAMPLE AS IT IS HEATED, THE
C   INTENSITY OF A SPECTRUM WILL CHANGE, INDEPENDENT OF WAVELENGTH OVER
C   THE SAME TEMPERATURE RANGE. THIS PROGRAM CORRECTS FOR THIS CHANGE
C   BY CALCULATING WHAT PERCENTAGE OF THE THERMOLUMINESCENCE (TL)
C   INTENSITY MUST BE ADDED TO MAKE THE TL INTENSITY APPEAR TO BE
C   CONSTANT.
C   THIS PERCENTAGE IS THEN ADDED TO THE SPECTRAL INTENSITY, WHICH
C   CORRECTS THE SPECTRA.
C
C   AUTHOR..  MICHAEL SHINN
C   INSTALLATION.. DEPARTMENT OF PHYSICS, OKLAHOMA STATE UNIVERSITY
C   DATE.. FEBRUARY 18, 1980
C   LANGUAGE.. A.N.S.I. STANDARD FORTRAN
C
C   INPUT..
C
C   N     = THE NUMBER OF DATA POINTS.
C   TEMP  = THE ARRAY OF TEMPERATURES (IN DEG. KELVIN) AT WHICH
C           DATA POINTS ARE TAKEN.
C   TLPMT = THE ARRAY OF VALUES OF THE TL PHOTOMULTIPLIER TUBE.
C   TLMAX = THE MAXIMUM VALUE OF TLPMT.
C   SPPMT = THE ARRAY OF VALUES OF THE SPECTRA PHOTOMULTIPLIER
C           TUBE, OVER THE SAME TEMPERATURES.
C
C   OUTPUT..
C
C   SPCOR = THE ARRAY OF CORRECTED SPPMT VALUES.
C
      DIMENSION TEMP(50),TLPMT(50),SPPMT(50),SPCOR(50)
C   ZERO THE ARRAYS.
      DO 1 J=1,50
       TEMP(J) = 0.0
       TLPMT(J) = 0.0
       SPPMT(J) = 0.0
       SPCOR(J) = 0.0
    1 CONTINUE
C   READ DATA FROM KEYBOARD.
      TYPE 2
    2 FORMAT(1H ,32HENTER THE NUMBER OF DATA POINTS.)
      ACCEPT 3,N
    3 FORMAT(I2)
      TYPE 4
    4 FORMAT(1H ,47HENTER THE TEMPERATURES AT WHICH DATA WAS TAKEN.)
      ACCEPT 5, (TEMP(J),J=1,N)
    5 FORMAT(F6.2)
      TYPE 6
    6 FORMAT(1H ,38HENTER THE CORRESPONDING TL PMT VALUES.)
      ACCEPT 7, (TLPMT(J),J=1,N)
    7 FORMAT(E15.7)
      TYPE 8
    8 FORMAT(1H ,44HENTER THE CORRESPONDING SPECTRAL PMT VALUES.)
      ACCEPT 9, (SPPMT(J), J=1,N)
    9 FORMAT(E15.7)
```

```
      TYPE 10
   10 FORMAT(1H ,61HENTER THE MAXIMUM VALUE OF TLPMT FOR THE
     *    PARTICULAR TL PEAK.)
      ACCEPT 11, TLMAX
   11 FORMAT(E15.7)
C
C   NORMALIZE TLPMT.
C
      DO 12 J=1,N
       TLPMT(J) = TLPMT(J)/TLMAX
   12 CONTINUE
C
C   CORRECT SPPMT.
C
      DO 13 J=1,N
       SPCOR(J) = SPPMT(J)/TLPMT(J)
   13 CONTINUE
C
C   WRITE VALUES OF SPCOR AND TEMP AND DISPLAY THEM GRAPHICALLY.
C
      TYPE 14
   14 FORMAT(1H0,2X,17HTEMP(DEG. KELVIN),5X,16HPMT CURRENT(AMP))
      TYPE 15, (TEMP(J),SPCOR(J), J=1,N)
   15 FORMAT(1H ,7X,F6.2,6X,E15.7)
      TYPE 16
   16 FORMAT(1H0,50X,44HROUGH PLOT OF TEMPERATURE VERSUS PMT CURRENT)
      CALL FRAMP(TEMP,SPCOR,N,6)
      STOP
      END
```

Subroutine FRAMP may be obtained from Dr. J. P. Chandler, Computing and Information Sciences, Oklahoma State University.

VITA

Michael David Shinn

Candidate for the Degree of

Master of Science

Thesis: THERMALLY STIMULATED LUMINESCENCE AND ELECTRON SPIN RESONANCE STUDIES IN ELECTRON-IRRADIATED $CaWO_4$

Major Field: Physics

Biographical:

Personal Data: Born in Stillwater, Oklahoma, September 6, 1956, the son of Oliver F. and Marilyn J. Shinn.

Education: Attended elementary and secondary schools in Bartlesville, Oklahoma; graduated from College High School May, 1974. Attended Oklahoma State University, majoring in Physics, minoring in Math and History; received a B.S. degree in Physics, July, 1978; completed requirements for Master of Science degree in Physics in July, 1980.

Professional Experience: Worked as Assistant to the Radiation Safety Officer with title of Graduate Research Assistant from 1978 to present.